Egypt. J. Chem. **Vol. 67** No. 4 pp. 559 - 576 (2024)

Egyptian Journal of Chemistry

http://ejchem.journals.ekb.eg/

Balanites aegyptiaca dates hydroethanolic extract shows anti-neurodegenerative effect in diabetes-mediated neurodegenerative disorders in rats.

Abeer Y. Ibrahim[1], Nermeen M. Shaffie[2], and Samah A. El-Newary[1*]

1 Department of Medicinal and Aromatic Plants Research, Pharmaceutical and Drug Industries Research Institute, National Research Centre, 33 El Bohouth St., Dokki, Giza 12622, Egypt.
2 Pathology Department, Medical Research and Clinical Studies Institute, National Research Centre, 33 El Bohouth St., Dokki, Giza 12622, Egypt.

Abstract

This study aimed to evaluate the potential application of *Balanites aegyptiaca* date hydroethanolic extract in treating diabetes-mediated neurodegenerative disorders in rats. Neurodegenerative disorders in diabetic male albino Wister rats were studied using a streptozotocin (STZ, 65 mg/kg body wt.) model. Rats orally received *Balanites* at 2250 mg/kg body wt. as ¼ LD_{50} for three months. Four groups were randomly organized: negative control, STZ control, extract control, and treated group. Results showed that the blood glucose level was reduced from 354.24±4.52 mg/dL (STZ group) to 115±4.92 mg/dL (treated group), which indicated that *Balanites* exhibited an anti-diabetic effect. Concomitantly, insulin significantly elevated (53.00% and 392.50%) compared with the STZ group ($P \leq 0.001$) after 45 and 90 days, respectively, with hypolipidemic action. Compared with the STZ group ($P \leq 0.001$), *Balanites* exerted a neurodegenerative repairing effect, as it significantly inhibited acetylcholinesterase (36.84% and 52.85%) based on acetylcholine content augmentation (28.40% and 53.14%) at the two follow-ups. In addition, *Balanites* ameliorated apoptosis, inflammation, oxidative stress, and neurotrophic factor in the brain. Brain sections showed no amyloid-beta plaque and neurofibrillary tangles that were recorded for the STZ group. Finally, *Balanites* addressed diabetes-induced neurodegenerative disorders in rats because of its orchestral approach mechanisms on acetylcholinesterase, amyloid-beta, neurofibrillary tangles, apoptosis, neuroinflammation, and oxidative stress.

Keywords: Diabetes-induced neurodegenerative disorders, Acetylcholine esterase, Amyloid-beta, Neurofibrillary tangles, Brain-derived neurotrophic factor (BDFN), Bcl-2.

Introduction

Neurodegeneration is a gradual deterioration of neurological function. It influences a large proportion of the universal population, particularly aging. Alzheimer's disease (AD) is the primary neurodegenerative disorder. WHO 2020 reported that AD and dementia account for about 17,957 or 3.23% of the total mortality in Egypt **[1].**

The sanitary human brain consists of billions of neuron-specialized cells that operate and transport information through electrical and chemical signals. These signals are sent among different brain parts from the brain to muscles or body organs. The brain usually shrunk without losing several neurons. In AD, the deterioration of brain neurons becomes prevalent, where a number of neurons lose their functions, such as communication, metabolism, and repair, and then die. Destructive neurons in the brain play a role in memory, including the entorhinal cortex and hippocampus. These neurons later affect the regions in the cerebral cortex responsible for language, reasoning, and social behavior. Consequently, several areas of the brain will be damaged. Over time, a person with AD progressively loses the ability to live independently. The brain histological sections of a person with AD is characterized by the (i) accumulation of hyperphosphorylated tau protein, (ii) abnormal level of beta-amyloid occurring and forming plaques, (iii) chronic inflammation represented as microglial activation, (iv) synaptic damage accompanied by neuronal loss, (v) increased activated genes, (vi) impaired energy metabolism, (vii) mitochondrial dysfunction, (viii) chronic oxidative stress, (ix) DNA damage, (x) dystrophic neurites, and (xi) vascular issues that affect brain blood vessels such as atherosclerosis and mini-strokes. Synaptic loss is a

*Corresponding author e-mail: samahelnewary@yahoo.com; (Samah A El-Newary).
Receive Date: 26 August 2023, Revise Date: 05 October 2023, Accept Date: 11 October 2023
DOI: https://doi.org/10.21608/ejchem.2023.231893.8501

strong correlate of cognitive impairment in patients with AD **[2- 4].**

Since 2000, the relationship between type 2 diabetes and cognitive disorders has been highlighted. However, in 2005, this field has been burst with novel information and novel notion, that is, primary brain insulin resistance and insulin insufficiency induced cognitive disorders and AD. Ample evidence shows that type-2 diabetes is related not only to vascular dementia but also to the clinical diagnosis of AD, which is a type of dementia. Some studies have shown that people with type-2 diabetes show reduced hippocampal and amygdala volumes and a threefold increased risk for medical temporal lobe atrophy compared with non-diabetic individuals. This idea was supported by the directory that tau gene expression and phosphorylation are organized by insulin and insulin-like growth factor signaling cascades **[5].**

In diabetes, oxidative stress also increases because of depletion in antioxidant capacity, which induce neuronal damage through mitochondrial dysfunction. Several studies have provided a potent directory propped of the postulate that AD appeared as a form of diabetes mellitus, which affected the brain. This knowledge is supported by the results obtained from experimental animals, in which rats with STZ-induced diabetes showed neuronal disorders. A small pilot study has demonstrated that intranasal insulin has some benefits to patients with early AD. Insulin bypasses the periphery and blood–brain barrier (BBB), reaching via extracellular bulk flow transport along olfactory and trigeminal perivascular channels and through traditional axonal transport pathways. Intranasal insulin administration could also improve human memory and attention without affecting plasma glucose levels **[5].** Several studies have proven that AD is intrinsically a neuroendocrine disease caused by eclectic impairments in insulin and insulin-like growth factor (IGF) signaling mechanics, including insufficiencies in local insulin and IGF expression **[6-7].**

The tested material in the current study is the hydroethanolic extract of *Balanites aegyptiaca* dates. *B. aegyptiaca*, which belongs to family *Balanitaceae*, is a widely distributed African plant of medicinal interest. Its fruit mesocarp is commonly used as an oral anti-diabetic drug in Egyptian folk medicine. *B. aegyptiaca* plant has many pharmacological effects, including anti-oxidative stress, anti-hypercholesterolemia, anti-cardiovascular diseases, hepatoprotective, and anti-hyperglycemia **[8].** Our previous *in vitro* study **[8]** has demonstrated that *B. aegyptiaca* date hydroethanolic extract had a potent anti-AD efficacy. This extract can inhibit acetylcholine and butyrylcholine esterase, which prevent neurotransmitter hydrolysis. In addition, it shows anti-tyrosinase activity, which is a neurofibrillary tangle former. In parallel, the extract has a selective inhibitory action on pro-inflammatory cytokine production rate-limiting enzyme COX-2. Furthermore, it exhibits potential antioxidant characteristics, lipid peroxidation inhibitory action, ROS and free-radical scavenging, reduction property, and metal chelation efficacy. Therefore, we incorporated *Balanites* extract in this preclinical study **[9]** to investigate it's *in vivo* anti-AD ability using $AlCl_3$-induced neurotoxicity in rats which proved that the date extract considerably reduced AD biomarkers, amyloid-beta (Aβ) and tau neurofibrillary tangle accumulation, and acetylcholinesterase activity. Apart from antioxidant and anti-inflammatory activities, this extract also exhibited significant activation of anti-apoptotic factor (Bcl-2) and neurotrophic factor (brain-derived neurotrophic factor, BDNF).

The current study aimed to evaluate the role of *Balanites* date hydroethanolic extract as anti-diabetic natural materials in protecting the brain from the progression of AD in diabetic cases using a rat model of STZ-induced diabetes.

Materials and methods

Chemicals

Streptozotocin was purchased from Sigma-Aldrich Company (St. Louis, MO, USA). Spectrophotometric kits were obtained from Biodigonestic Egypt, Dokki, Giza, Egypt. ELISA kits of cholinesterase biomarkers (acetylcholine concentration (Cat No.: SL0027Ra) and cholinesterase (Cat No.: SL0027Ra) activity) were purchased from Sunlog Biotech Co., Ltd, China, SALES@SUNLONGBIOTECH.COM. Insulin (Cat No.: ER1113), glucagon (Cat No.: ER1594), Bcl-2 (Cat No.: ER0762), IL15 (Cat No.: ER1915), and BDNF (Cat No.: ER0008) ELISA kits were obtained from Wuhan fine Biotech Co., Ltd, *China,* Email: *fine*@fn-test.com.

Plant collection and extraction

Dates of *B. aegyptiaca* were collected from Aswan at a mature stage and were authenticated by Prof. Dr. Kamal Zaied (Plant Taxonomy, Faculty of Science, Cairo University, Egypt).

The pulp (fruit without seeds) was dried, and the dried powder (1 kg) was exhaustively extracted with 70% ethanol by shaking soaking at room temperature. Filtrates were collected and evaporated under reduced pressure. The remaining extract was

then lyophilized, and the obtained powder was kept at -20°C until use **[8]**.

Animals and accommodation

Animals and diet were obtained from the Animal House of National Research Centre, Egypt. Adult male albino rats (100 rats, weighting 150-180 g) were used. Rats were fed on a standard diet and maintained under laboratory conditions, temperature-controlled at 25±2°C, relative humidity 60±5%, and light/dark cycles (12/12 h). Animals were housed in polypropylene cages.

Determination of the acute toxicity study

According to the OCDE guideline for testing chemicals **[10]**, acute toxicity study of the extract was performed. Male albino mice (n= 8) were tested by administering the extract at different doses in an oral route by increasing or decreasing the dose according to the animal's response (1,000 to 10,000 mg/ kg). All groups were monitored for any gross effect or mortality for 48 h and considered for 14-days. *Balanites* extract was safe until 9 g/ kg body weight.

Evaluation of the neuronal protection efficacy of *Balanites* hydroethanolic extract in relation to its anti-diabetic effect.

Chemically induced diabetes model in male rats

Age-matched normal rats received an equivalent volume of normal saline. According to Abdel-Haleem et al. **[11]**, rats were fasted overnight and then intraperitoneally injected with STZ (65 mg/ kg B.wt.) in 0.1 mol/l citrate buffer (pH 4.5). Rats were administered glucose (25%) after one hour of STZ injection and were kept on glucose (5%) overnight to overcome STZ-induced hyperglycemia. One week after STZ injection, blood samples were collected through the tail vein, and plasma glucose level & insulin level were measured by plasma glucose enzymatic kits and insulin ELISA kit, respectively. Rats with plasma glucose level ≥ 300 mg/ dl and symptoms of polyuria, polyphagia, and polydipsia were considered diabetic and were used in the current study. The fasting plasma insulin levels in STZ-induced diabetic rats were 1.32 ± 0.6 pmol/ l, which is markedly lower than normal rat level (166.2± 4.3 pmol/ l).

Experimental design of neuronal protection by anti-diabetic materials

Extract dose was defined as ¼ the LD_{50} of the extract that determined in the current study. Rats received extract orally by stomach tube.

After adaption for one week, 80 animals were divided into four groups as follows:

Group I: 20-rats received 1 ml saline solution for three months in an oral route. They were kept as a negative control.

Group II: 20-rats received *Balanites* hydroethanolic extract orally at 2250 mg/ kg body weight (25% LD_{50}) for three months. These rats were served as extract control group.

Group III: 30-diabetic rats that were intraperitoneally injected with STZ (65 mg/ kg body wt. in a 0.1 mol/ l citrate buffer pH 4.5) received 1 ml saline solution for three months. These rats were maintained as STZ group.

Group VI: 30-diabetic rats that were intraperitoneally injected with STZ (65mg/ kg body wt. in a 0.1 mol/ l citrate buffer pH 4.5) then they were received *Balanites* extract orally at 2250 mg/ kg body weight for 90 days. These rats were served as a treated group.

Rats were followed up every 45 days with five animals. Rats were fasted overnight and were subjected to anesthesia for collection of blood samples and vital organs. Rats were anesthetized by ketamine injection (87 mg/ kg body weight) and xylazine (13 mg/ kg) dissolved in normal saline with simultaneously i.p. injection each rat received 0.2 ml/ 100 g body weight **[12]**. Blood samples were collected from the retro-orbital plexus and were centrifuged at 4000 *g* for 10 min to separate sera. The whole-brain of each rat was rapidly dissected, washed with isotonic saline, and dried on filter paper. The brain of each rat was weighed and was divided into two portions; the first was used in histopathological investigations, whereas the other was homogenized to give 10% (w/v) homogenate in an ice-cold medium containing 50 mM Tris-HCl and 300 mM sucrose at pH 7.4. The homogenate was centrifuged at 4°C. The supernatant was stored at -80°C and was used in biochemical analyses. Vital organs (heart, lungs, liver, kidneys, spleen, and testis) were harvested from sacrificed rats which were carefully examined for gross lesions and weighed (Precisa digital weighing balance, Type 300-

9213/E 125A, Switzerland). The weight of each organ was standardized to 100 g of body weight.

Biochemical assessment

Liver enzymes activities were spectrophotometrically assessed; alkaline phosphatase (ALP) **[13]**, aspartate aminotransferase (AST), and alanine aminotransferase (ALT) **[14]**, in sera. Meanwhile, according to Henry **[15]** and Doumas et al. **[16]**, total protein and albumin were determined. Globulin was calculated by the difference between total protein and albumin **[17]**.

Kidney function biomarkers: urea, uric acid, and creatinine, were estimated spectrophotometrically in sera **[18-20]** respectively.

Lipid profile including total cholesterol (TC), high-density lipoprotein cholesterol (HDL-C), triglycerides (TG), and total lipid (TL), were spectrophotometrically assessed according to Allain et al. **[21]**; Naito and Kaplan **[22]**; Fossati and Prencipe **[23]**; Estadella et al. **[24]** whereas low-density lipoprotein cholesterol (LDL-C), and very-low-density lipoprotein cholesterol (VLDL-C), were calculated based on Friedewald et al. **[25]**; Naito and Kaplan **[22]**.

Oxidative stress biomarkers including nitric oxide (NO), hydrogen peroxide H_2O_2, and malondialdehyde (MDA) were spectrophotometrically measured in brain homogenate according to Montgomery and Dymock **[26]**; Chance and Maehly **[27]**; Ohkawa et al. **[28]**.

Antioxidant brain biomarkers including reduced glutathione (GSH), glutathione reductase (GR), glutathione *S*-transferase (GST), glutathione peroxidase (GPx), catalase (CAT), and superoxide dismutase (SOD) were estimated according to Griffith, 1980 **[29]**; Goldberg and Spooner **[30]**; Paglia and Valentine **[31]**; Habig et al. **[32]**; Beers and Sizer **[33]**; Fridovich **[34]**, sequentially.

Cholinesterase biomarker (acetylcholine concentration and cholinesterase activity), an inflammatory biomarker (IL-15), apoptotic factor, and anti-apoptosis were determined according to the brochure of ELISA kits. Brain total protein concentration was measured for calculation of enzyme-specific activity **[35]**. The assessments were done using ELISA (Asus expert from austria).

Histopathological studies

Specimens of all animals were dissected immediately after death and fixed in 10% neutral-buffered formalin saline for at least 72 h. Sections were stained with hematoxylin-eosin and then were investigated using a light microscope (CX 41, Olympus, Tokyo, Japan) **[36]** for histopathological investigations.

Immunohistochemical studies

Immunostaining was performed as described by **Murayama et al., [37] and Shin et al., [38].** Immunostaining of paraffin-embedded brain sections was performed using the polyclonal Aβ antibody (Anti-Amyloid β (Aβ) x-40, clone 11A5-B10- EMD Millipore Corporation, 28820 Single Oak Drive, Temecula, CA 92590 USA) in concentration 1:250. Antigen retrieval was performed via heating in a microwave oven (25 min at 720 W). Then, sections were immersed in 1% hydrogen peroxide in methanol for 5 min. Sections were incubated with primary antibodies at 4°C overnight, with the secondary antibodies for about 1 h at room temperature.

Sections of the pancreas were stained by an anti-insulin antibody (Rabbit anti-insulin antibody - SL0855R- Sun Long Biotech Co., LTD). Immunohistochemistry for insulin was performed similarly using a concentration of (1:400-800 dilution) overnight at 4°C. After washing with PBS, a secondary antibody (1:200 dilution; Dako) was used for 30 min at room temperature. Samples were counterstained with H&E for 2–3 min.

Statistical Analysis

Results were presented as mean ± SD (n= 6). Data were analyzed by BIM-SPSS 25.0 software. To compare differences between the means of multiple groups, a one-way analysis of variance (ANOVA) followed by Tukey's *post hoc* test was used. $P \leq 0.001$ was considered to indicate statistical significance. In addition, all groups were compared to the negative group, whereas the treated group was compared to the STZ-group and -ve control.

Results

Diabetes was induced in male rats using a streptozotocin (STZ) model. The diabetic animals were treated with reported anti-diabetic materials, *Balanites* date hydroethanolic extract, as anti-AD agent.

Anti-diabetic effect of Balanites date hydroethanolic extract

Five biomarkers were determined to evaluate the anti-diabetic efficacy of *Balanites* on rats with STZ-induced diabetes, including animals' weight, blood glucose concentration, serum insulin, serum glucagon, and lipid profiles.

Blood glucose concentration

Blood glucose concentration was determined after 7, 14, 21, 28, 45, and 90 days **(Table 1)**. Administering STZ magnified glucose concentration

in the STZ group, 345.25, 357.82, 364.79, 359.71, 361.24, and 354.24 mg/ dL compared to the negative group. Meanwhile, the blood glucose level of the treated group was significantly reduced by approximately 52.21%, 58.75%, 67.23%, 66.33%, 67.56%, and 66.41% compared with the STZ group ($P \leq 0.001$).

Serum insulin and glucagon concentration

STZ administration significantly depleted serum insulin concentration to 2.00 ± 0.15 and 0.80 ± 0.004 U/ dL at 1st and 2nd follow-up, respectively, with a significant increase in serum glucagon (50.61 ± 2.18 and 66.51 ± 1.17 pg/ mL at 1st and 2nd follow-up, respectively) compared with the negative control ($P \leq 0.001$, **Fig. 1**). Serum insulin and glucagon concentration of treated rats showed an opposite trend in the STZ group. *Balanites* extract produced elevation in serum insulin levels in the treated group (3.06 ± 0.11 and 3.94 ± 0.34 U/ dL at 1st and 2nd follow-up, respectively); meanwhile, serum glucagon levels were significantly declined by about 45.17% and 62.35% compared with the STZ group at the two follow-ups.

Serum insulin and glucagon levels of the extract group were close to those of the negative control. Interestingly, *Balanites* restored the serum insulin and glucagon concentrations of the treated group near to those of the negative control, particularly at 2nd follow-up.

Table 1 Glucose following up of diabetic animals treated with *Balanites* extract through the experimental period.

Groups \ Following up time (days)	7	14	21	28	45	90
Negative group	111.32±2.31	109.82±2.48	113.11±2.16	110.42±6.18	114.31±5.26[a]	111.27±6.78 [b]
STZ-group	342.51±3.66*	357.82±3.64*	364.79±3.54*	359.71±7.01*	361.24±7.11*	354.24±4.52*
Treated-group	165.00±1.60**	147.61±3.48**	119.55±3.18**	121.11±8.12**	117.15±6.21 [a]**	115±4.92 [b]**

All groups were compared to the negative group, whereas the treated group was compared to the STZ-group and negative group. The appearance of * means a significant difference compared to -ve control, while the appearance of ** means a significant difference compared to the disease group. Groups that have the same letter showed an insignificant difference between them.

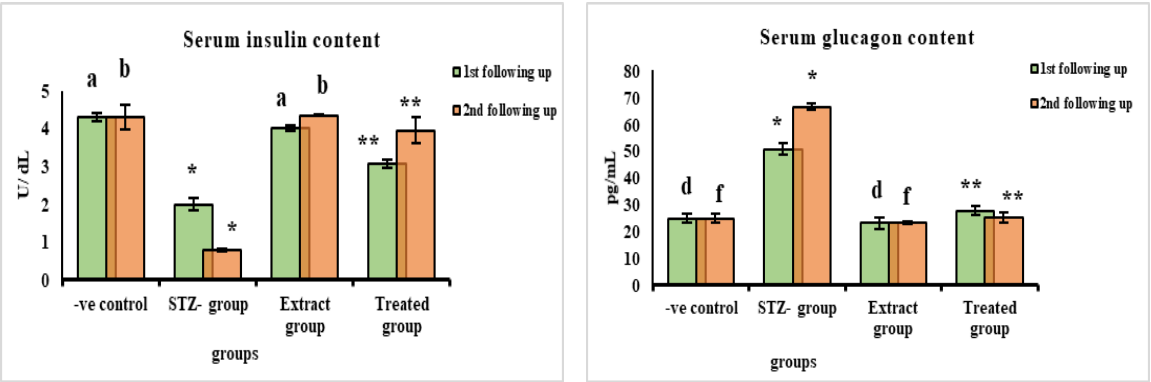

Fig. 1 *Balanites* extract a potential role in serum insulin and glucagon levels of STZ-induced diabetes in animals.

Data are presented as the meaning of six animals. The appearance of * means a significant difference compared to the negative group, while the appearance of ** means a significant difference compared to the STZ group. Groups that have the same letter showed an insignificant difference between them.

Serum lipid profiles

STZ administration was accompanied by hyperlipidemia features found in the amplified lipid profile, including TL, TC, TG, and VLDL-C, which were increased by about 39.85%, 32.70%, 219.01%, and 219.01% compared with the negative group at the 1st follow-up. At the 2nd follow-up, the lipid profile continuously increased (46.46%, 45.55%, 257.21%, and 257.21% for TL, TC, TG, and VLDL-C, respectively) compared with the negative control **(Fig. 2)**. On the contrary, HDL-C was significantly reduced to 7.92 ± 0.24 and 6.45 ± 0.26 mg/ dL at 1st and 2nd follow-ups. *Balanites* extract exhibited a

hypolipidemic action. It significantly reduced TL (28.04% and 41.42%), TC (20.20% and 34.70%), TG and VLDL-C (38.73% and 52.23%), and LDL-C (44.80% and 63.27%) at the 1st and 2nd follow-up compared with the STZ group. Meanwhile, the HDL-C level of the treated group increased by about 121.21% and 177.98% at the two follow-ups compared with the STZ group. All determined lipid profile parameters of the treated group were improved remarkably to be close to the values of the negative group, except for the TG level, at the two follow-ups.

Balanites administration showed a hypolipidemic action in the positive group compared with the negative group. All lipid profile parameters of the positive group were less than those of the negative group in the two follow-ups, except for the HDL-C level.

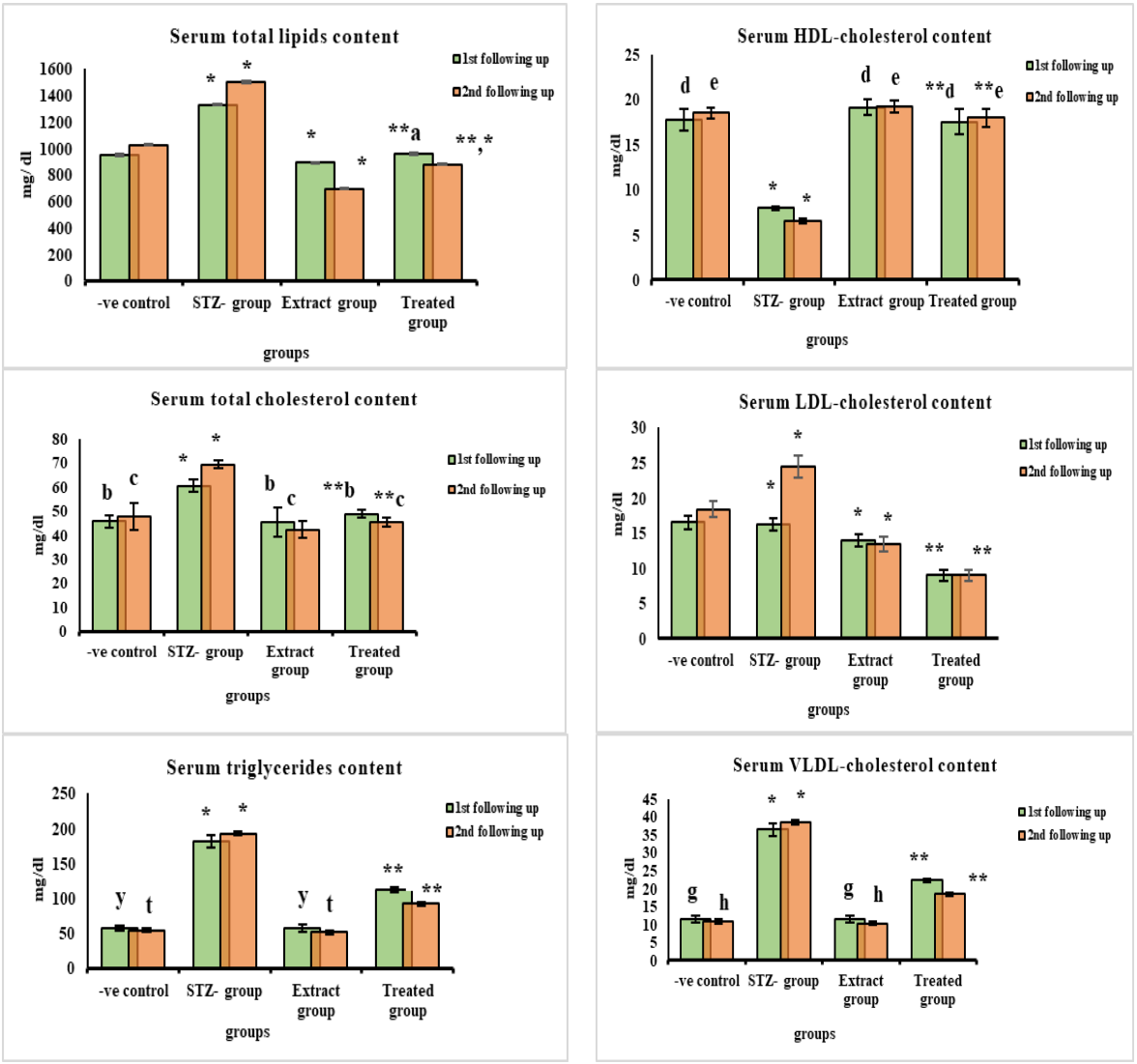

Fig. 2 Effect of *Balanites* extract on lipid profile biomarkers in STZ-induced diabetes in male rats.

Data are presented as the meaning of six animals. The appearance of * means a significant difference compared to the negative group, while the appearance of ** means a significant difference compared to the STZ group. Groups that have the same letter showed an insignificant difference between them.

Animal weight and relative weight of brain and pancreas

The weight of rats receiving STZ dramatically decreased to 120.00 ± 1.68 and 81.31 ± 1.24 g at 1st and 2nd follow-up, respectively, compared with the negative group ($P \leq 0.001$, **Fig. 3A).** The rates of the treated group were normally grown to 202.17 ± 1.29 and 238.07 ± 1.36 g at 1st and 2nd follow-up, where they significantly increased by about 68.48% and 192.80% compared with the STZ group. On the contrary, rats of the extract group were normally grown compared with the negative group.

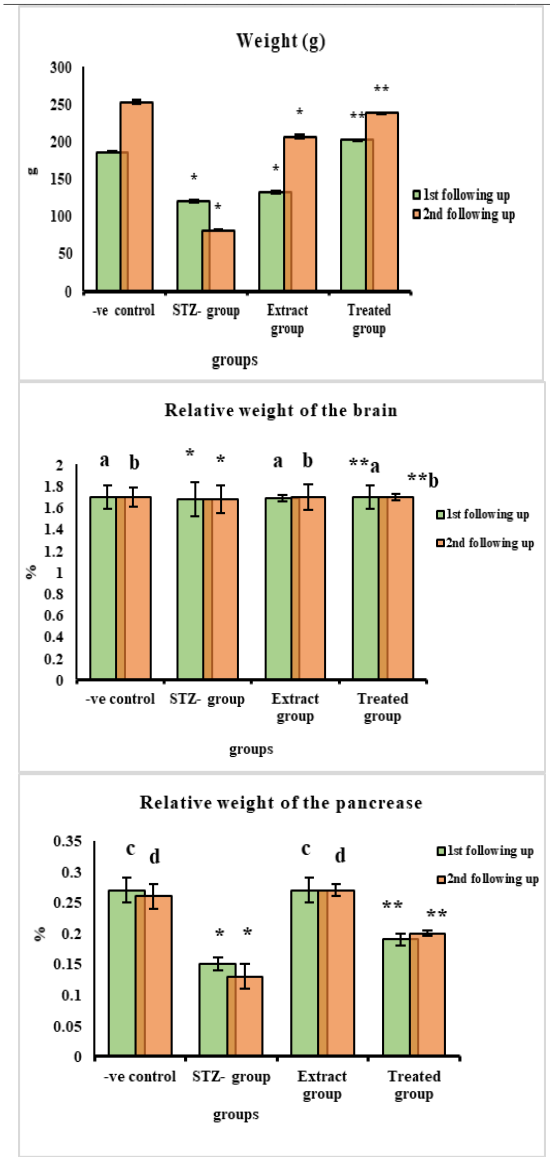

Fig. 3 Effect of *Balanites* extract on weight (A), the relative weight of brain (B) and pancreas (C) in STZ-induced diabetes in male rats.

Data are presented as the meaning of six animals. The appearance of * means a significant difference compared to the negative group, while the appearance of ** means a significant difference compared to the STZ group. Groups that have the same letter showed an insignificant difference between them.

The relative weight of pancreas shrunk at the 1st and 2nd follow-up compared with the negative group ($P \leq 0.001$). Reversely, the relative weight of the pancreas of treated group was significantly increased from 0.15% ± 0.01% and 0.13% ± 0.02% in the STZ group to 0.19% ± 0.01% and 0.20% ± 0.004% in the treated group at 1st and 2nd follow-ups, respectively **(Fig. 3C).** The relative weight of the brain was insignificantly affected by STZ or *Balanites* administration at the two follow-ups **(Fig. 3B)**.

The ameliorative effect of Balanites date hydroethanolic extract on the safety profile.

The safety profile of the extract group and treated animals was evaluated, including the relative weight of vital organs (**Supplementary Table 1**) and liver (**Supplementary Table 2**) and renal functions (**Supplementary Table 3**) in the two follow-ups, and it was compared with the negative control. STZ administration caused harmful changes that were considered as hepatotoxicity and nephrotoxicity whereas Balanites extracts administration appeared safe characters.

The ameliorative effect of Balanites date hydroethanolic extract on diabetes-induced neurodegeneration disorders.

This study was performed to evaluate the ability of *Balanites* to treat neuro-complications in diabetes mellitus. Five biomarkers related to neurodegeneration-associated diabetes were studied, including the (i) state of neurotransmitters (AChE activity and ACh content), (ii) apoptotic condition (anti-apoptotic factor; BCl-2), (iii) brain growth factor (BDNF), (iv) neuroinflammation position (pro-inflammatory; IL-15), and (v) oxidative stress.

Neurotransmitters

Diabetic induction was accompanied by a degree of neurodegeneration, where AChE was dramatically activated, decomposing Ach, which depleted remarkably **(Fig. 4A and B).** The AChE activity in the STZ group was significantly activated at the 1st (1175.35 ± 4.18 U/mg protein) and 2nd (1394.27 ± 5.11 U/ mg protein) follow-up compared with the negative group (809.00 ± 4.16 and 810.06 ± 3.16 U/ mg protein, respectively), $P \leq 0.001$. In the STZ group, the AChE activity significantly decreased the ACh content reaching $5.6 \times 10^{-2} \pm 0.002$ and $5.10 \times 10^{-2} \pm 0.002$ nmol/ mg protein compared with the negative group ($7.88 \times 10^{-2} \pm 0.001$ and $7.9210^{-2} \pm 0.001$ nmol/ mg protein, respectively).

Balanites showed an anti-AChE activity, where AChE of the treated group was significantly minimized to 742.34 ± 6.18 and 657.41 ± 2.57 U/ mg protein, with 36.84% and 52.85% reduction at the two follow-ups compared with the STZ group. Based on the AChE inhibition of the treated group, the ACh content was significantly augmented to $7.19 \times 10^{-2} \pm 0.002$ and $7.81 \times 10^{-2} \pm 0.001$nmol/ mg protein, with 28.40% and 53.14% increment compared with the STZ group at the two follow-ups. *Balanites* significantly inhibited AChE activity that significantly induced ACh content compared with the negative control.

In addition, *Balanites* exhibited an anti-AChE efficacy in the extract control group. In the two follow-ups, AChE activity was significantly diminished (8.24% and 18.84%), and the ACh content

was remarkably increased (5.84% and 14.90%) compared with the control group, the effect was time dependent.

A

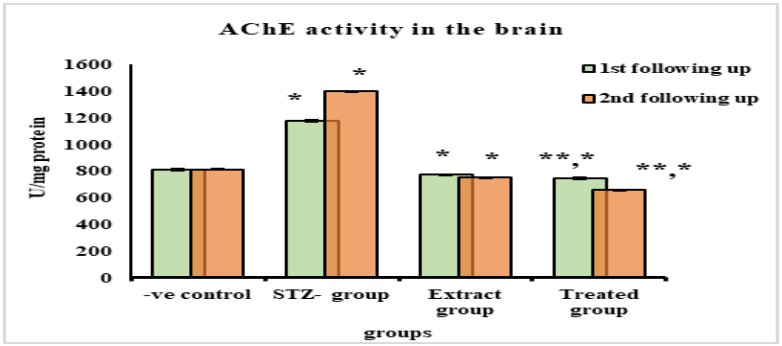

B

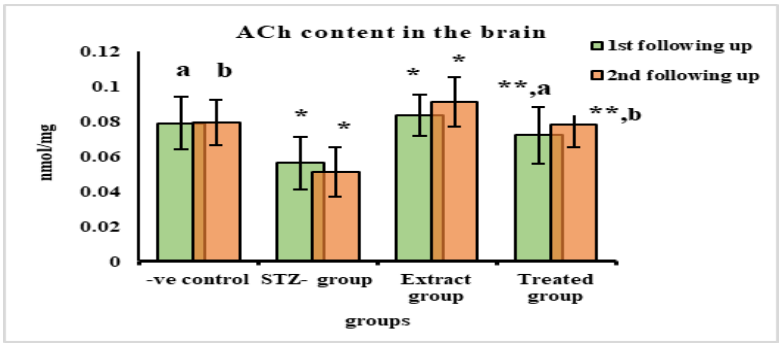

C

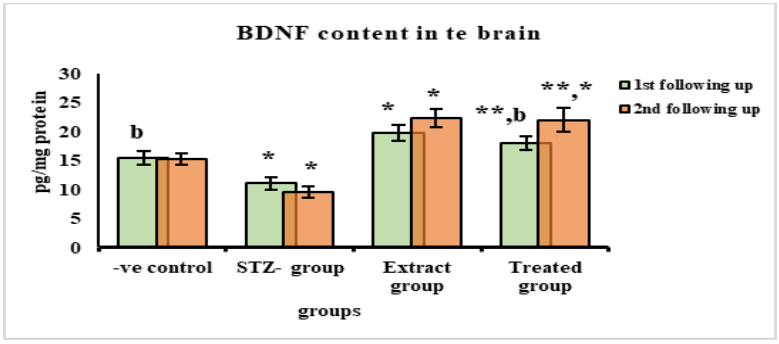

D

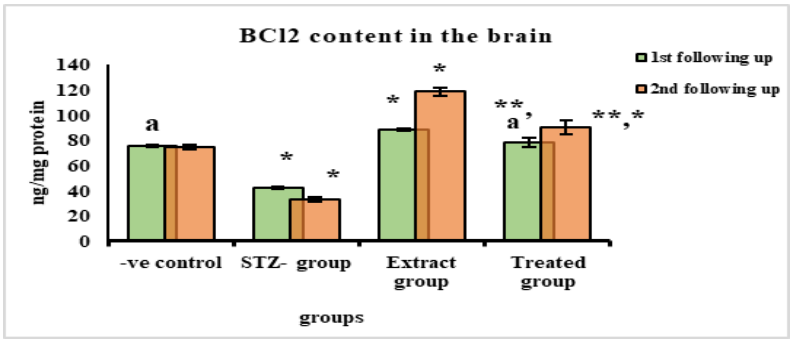

E

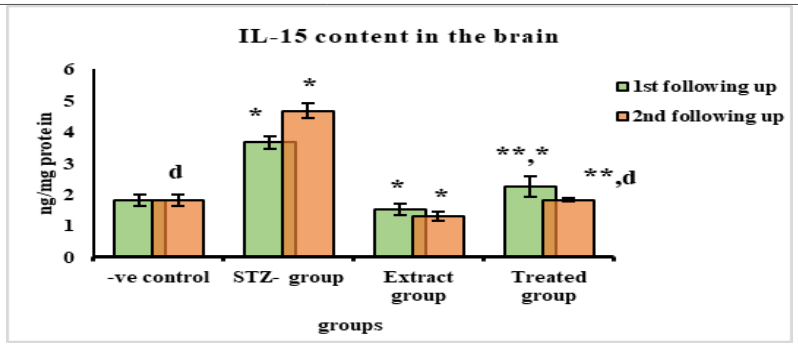

Fig. 4 The ameliorative effect of *Balanites* extract on neurotransmitters degradation (A& B) brain neurotrophic factor (C), Bcl 2 (D), and IL-15 (D) in brain tissue of STZ-induced diabetic rats.

Data are presented as the meaning of six animals. The appearance of * means a significant difference compared to the negative group, while the appearance of ** means a significant difference compared to the STZ group. Groups that have the same letter showed an insignificant difference between them.

Neurotrophic factor

BDNF is a growth factor in the mammalian brain that plays a vital role in facilitating nerve growth and maturation through development stages and regulating synaptic transmission and plasticity in adulthood.

BDNF was significantly affected by STZ administration. It was withdrawn to 11.01 ± 1.01 pg/ mL at the 1st follow-up and then retired to 9.53 ± 0.93 pg/ mL at the 2nd follow-up, compared with the negative control, which remained stable at the two follow-ups ($P \leq 0.001$, **Fig. 4C**).

The opposite trend was recorded in the treated group. *Balanites* administration increased BDNF in the treated group (62.76% and 130.22% increment) than the STZ group at the two assayed times. BDNF was amplified to 17.92 ± 1.18 and 21.94 ± 2.08 pg/ mL at the 1st and 2nd follow-up compared with the STZ group. In addition, the BDNF of the treated group was higher than that of the negative group at the two follow-ups.

Balanites significantly augmented BDNF in the extract group by about 27.75% and 46.58% at the two follow-ups compared with the negative group.

Anti-apoptotic Bcl-2

Anti-apoptotic factor Bcl-2 was significantly depleted regarding STZ administration and was diminished time dependently (42.05 ± 1.19 and 33.16 ± 1.56 ng/ mg protein), as compared with the negative control (75.42 ± 1.16 and 74.68 ± 1.89 ng/ mg protein) at 1st and 2nd follow-ups, respectively **(Fig. 4D).**

On the contrary, *Balanites* restored Bcl-2 in the treated group toward normalization. It significantly progressed time dependently to reach 78.15 ± 1.89 and 90.07 ± 5.29 ng/ mg protein, accounting for +85.85% and +171.62% at the 1st and 2nd follow-up, respectively, compared with the STZ group. Furthermore, BDNF of the treated group was two times that of the negative group.

A significant increase in BDNF in the extract group was recorded (+17.13% and 58.33% at the 1st and 2nd follow-up compared with the negative group.

Anti-inflammatory interleukin (IL-15)

Inflammation was associated with STZ administration, as shown in the elevation of the pro-inflammatory cytokine (IL-15). In the STZ group, IL-15 significantly increased to 3.65 ± 0.21 ng/ mg protein (+100.55%) at the 1st follow-up and to 4.66 ± 0.23 ng/ mg protein (+157.46%) at the 2nd follow-up, whereas the negative group remained stable around 1.82 ng/ mg protein **(Fig. 4E).**

Meanwhile, IL-15 in the treated group was considerably minimized to 2.24 ± 0.32 ng/ mg protein (−38.63%) at the 1st follow-up and to 1.82 ± 0.05 ng/ mg protein (−60.94%) at the 2nd follow-up, compared with the STZ group ($P \leq 0.001$). *Balanites* reconstituted IL-15 in the treated group toward normalization. This result was close to the negative group at the 2nd follow-up (1.82 ± 0.05 and 1.81 ± 0.18 ng/ mg protein, respectively).

Balanites showed an anti-inflammatory potential. It significantly reduced IL-15 in the extract group to reach less value than the negative control (16.48% and 28.73% decrease at the 1st and 2nd follow-ups, respectively).

The anti-oxidative effect of Balanites date hydroethanolic extract on diabetes-oxidation disorders.

The ability of *Balanites* to recruit oxidative stress was investigated in three mechanisms, including (i) reducing oxidative stress biomarkers (MDA, NO, and H_2O_2), (ii) inducing a non-enzymatic antioxidant biomarker (GSH), and (iii) activating antioxidant enzymes (GR, GST, GPx, SOD, and CAT).

Oxidative stress

STZ administration significantly induced oxidative stress biomarkers compared with the

negative group ($P \leq 0.001$). In the STZ group, (i) lipid peroxidation was promoted, where MDA was significantly increased (29.04% and 59.75%); (ii) ROS production was induced, (iii) H_2O_2 was amplified (26.32% and 48.57%), and (iv) NO production was considerably increased (87.43% and 130.81%) at 1st and 2nd follow-ups compared with the negative control **(Table 2)**.

Conversely, *Balanites* remarkably neutralized oxidative stress biomarkers compared with the STZ group. In the treated group, (i) lipid oxidation was suppressed, and MDA level was considerably depleted (15.26% and 40.25%); (ii) H_2O_2 concentration was significantly minimized (9.47% and 35.90%), and (iii) NO was significantly suppressed (14.25% and 50.12%) compared with the STZ group at the two assayed times. Moreover, *Balanites* restored MDA, H_2O_2, and NO concentrations in the treated group close to the negative control.

Rats in the extract control group produced MDA, H_2O_2, and NO equal to those of the negative group in the two follow-ups.

Table 2

Oxidative stress characteristics of the brain in STZ-induced diabetes in animals treated with *Balanites* extract.

Group / Parameter		-ve control	Positive controls		Treated group
			STZ-group	Extract group	
MDA (nmol/mg tissue)	1st following up	3.96±0.57	5.11±0.62*	3.71±0.29*	4.33±0.16**
	2nd following up	3.95±0.92	6.31±0.13*	3.36±0.22*	3.77±0.22**
NO (µmol/mg tissue	1st following up	1.91±0.31[a]	3.58±0.17*	1.91±0.04[a]	2.07±0.34**[a]
	2nd following up	1.85±0.23[b]	4.27±0.26*	1.83±0.06[b]	2.13±0.16**,*
H_2O_2 (nmol/mg tissue)	1st following up	4.18±0.13	5.28±0.33*	3.48±0.11*	4.78±0.28**,*
	2nd following	4.20±0.11	6.24±0.14*	3.94±0.31*	4.00±0.13**, *

All groups were compared to the negative group, whereas the treated group was compared to the STZ-group and negative group. The appearance of * means a significant difference compared to -ve control, while the appearance of ** means a significant difference compared to the disease group. Groups that have the same letter showed an insignificant difference between them.

Antioxidant biomarkers

STZ administration was accompanied with significant depletion in antioxidant biomarkers at the two assayed times. The STZ group showed minimized GSH (0.69 ± 0.03 and 0.59 ± 0.01 mg/ dL) at the two follow-ups as compared with negative control **(Table 3).**

Meanwhile, rats of the treated group produced GSH higher than the STZ group (169.57% and 238.98% increase) at the two assayed times. Insignificant difference in GSH concentration was observed between the extract and negative groups.

By contrast, the STZ group suppressed antioxidant enzymes. At the 1st follow-up, GR, GST, GPx, SOD, and CAT activities were statistically suppressed by about 28.47%, 55.25%, 64.95%, 39.83%, and 34.78%, respectively, compared with the negative control ($P \leq 0.001$). However, at the 2nd follow-up, the deleterious effect of STZ was increased, and enzymes were inhibited (47.88%, 58.80%, 70.41%, 45.66%, and 52.17% for GR, GST, GPx, SOD, and CAT inhibition, respectively) compared with the negative group.

Balanites significantly activated antioxidant biomarkers in the treated group compared with the STZ group ($P \leq 0.001$). Antioxidant enzymes in the treated group were stimulated considerably, including GR (38.29% and 89.63%), GST (137.04% and 166.67%), GPx (179.41% and 279.31%), SOD (60.97% and 92.68%), and CAT (53.33% and 136.36%) at the 1st and 2nd follow-up, respectively, compared with the STZ group. However, differences in GR, GPx, and CAT activities between the treatment and negative groups in the two follow-ups were insignificant.

Therefore, the antioxidant biomarkers in the extract control group were significantly activated to reach more activity compared with the negative group in the two follow-ups.

Table 3

Effect of *Balanites* extract on antioxidant status of brain in STZ-induced diabetes in rats.

Group / Parameter		-ve control	Positive controls		Treated
			STZ-group	Extract group	
GSH (mg/dL)	1st following up	1.93±0.11	0.69±0.03*	2.21±0.01*	1.86±0.15**
	2nd following up	1.91±0.11	0.59±0.01*	2.36±0.00*	2.00±0.24**
GR (U/ mg protein/min.)	1st following up	7.34±0.67[a]	5.25±0.38*	7.95±0.78 [a]	7.26±0.46** [a]
	2nd following up	7.77±0.68 [b]	4.05±0.12*	8.34±0.96*	7.68±0.31** [b]
GST (U/ mg protein/min.)	1st following up	1.81±0.08	0.81±0.02*	2.03±0.08*	1.92±0.14**,*
	2nd following up	1.82±0.09	0.75±0.01*	2.23±0.34*	2.00±0.56**,*
GPx (U/ mg protein/min.)	1st following up	0.97±0.03 [c]	0.34±0.01*	1.15±0.11*	0.95±0.11**, [c]
	2nd following up	0.98±0.06	0.29±0.02*	1.34±0.10*	1.10±0.22**,*
SOD (U/ mg protein/min.)	1st following up	8.26±0.75	4.97±0.31*	9.86±1.17*	6.00±1.22**,*
	2nd following up	8.30±0.99	4.51±0.23*	11.27±0.91*	7.21±0.88**,*
CAT (U/ mg protein/min.)	1st following up	0.23±0.06 [h]	0.15±0.01*	0.27±0.03*	0.23±0.01**, [h]
	2nd following up	0.23±0.01	0.11±0.01*	0.29±0.03*	0.25±0.02**, *

All groups were compared to the negative group, whereas the treated group was compared to the STZ-group and negative group. The appearance of * means a significant difference compared to -ve control, while the appearance of ** means a significant difference compared to the disease group. Groups that have the same letter showed an insignificant difference between them.

Histopathological examinations

Interestingly, the administration of STZ has a harmful effect on neuron cells, including the shrinking of neurons, dark pyknotic nuclei, and undefined nucleoli **(Fig. 5 [part I], B)**, indicating that the induction of an apoptotic effect could lead to neuronal death, which supports the hypothesis of considering the diabetic condition in neurodegeneration induction and progression. Sections of the animal brain administered with *Balanites* date aqueous extract demonstrated that this extract is safe on brain tissue until the end of the experimental period (90 days), as they showed the normal structure of cerebral cortex tissue **(Fig. 5 [part I], C)**. Based on the diabetic sections, *Balanites* partially recovered some degenerated cells **(Fig. 5 [part I], D)**, and death cell order is presented in few apparent neuronal dead cells. *Balanites* might show their protection directly to brain tissue through the anti-diabetic effect.

The above-mentioned figure indicated the safety of the tested material on the hippocampus, as they showed normal cell appearance **(Fig. 5 [part II], C)**. The results of the hippocampal section showed the same trend as the results of the cortex section, which supported the neuronal protection of the anti-diabetic material (*Balanites*). The photomicrograph section of the hippocampus in intoxicated animals treated with the tested material showed the potent anti-AD effect of *Balanite*s, which appears to be normal in most cells.

The aforementioned results of the pancreatic section of STZ-treated animals showed a toxic effect on the pancreas based on the reduction in Langerhans islets with apoptotic formation **(Fig. 6 [part I], B)**. Such sections also showed the safety of the tested balanites extract administration over the experimental period (90 days: **Fig. 6 [part I], C)**. Balanites extract showed a curative effect on STZ-treated animals with different therapeutic levels. *Balanites* also showed improvement, that is, the marked amelioration in structure and size of Langerhans islet is returning to normality.

The liver of animals was also investigated as part of the safety profile administration of the Balanites extract and considered as a susceptible organ for diabetes conditions. STZ injection showed dilatation of blood vessels and karyolysis of hepatocytes, indicating that cytotoxicity leads to cell death **(Fig. 6 [part II], B)**. The administration of Balanites extract showed a typical structure during 90 days of treatment, except for slight blood vessel congestion with *Balanites* extract, confirming the safe use of tested materials.

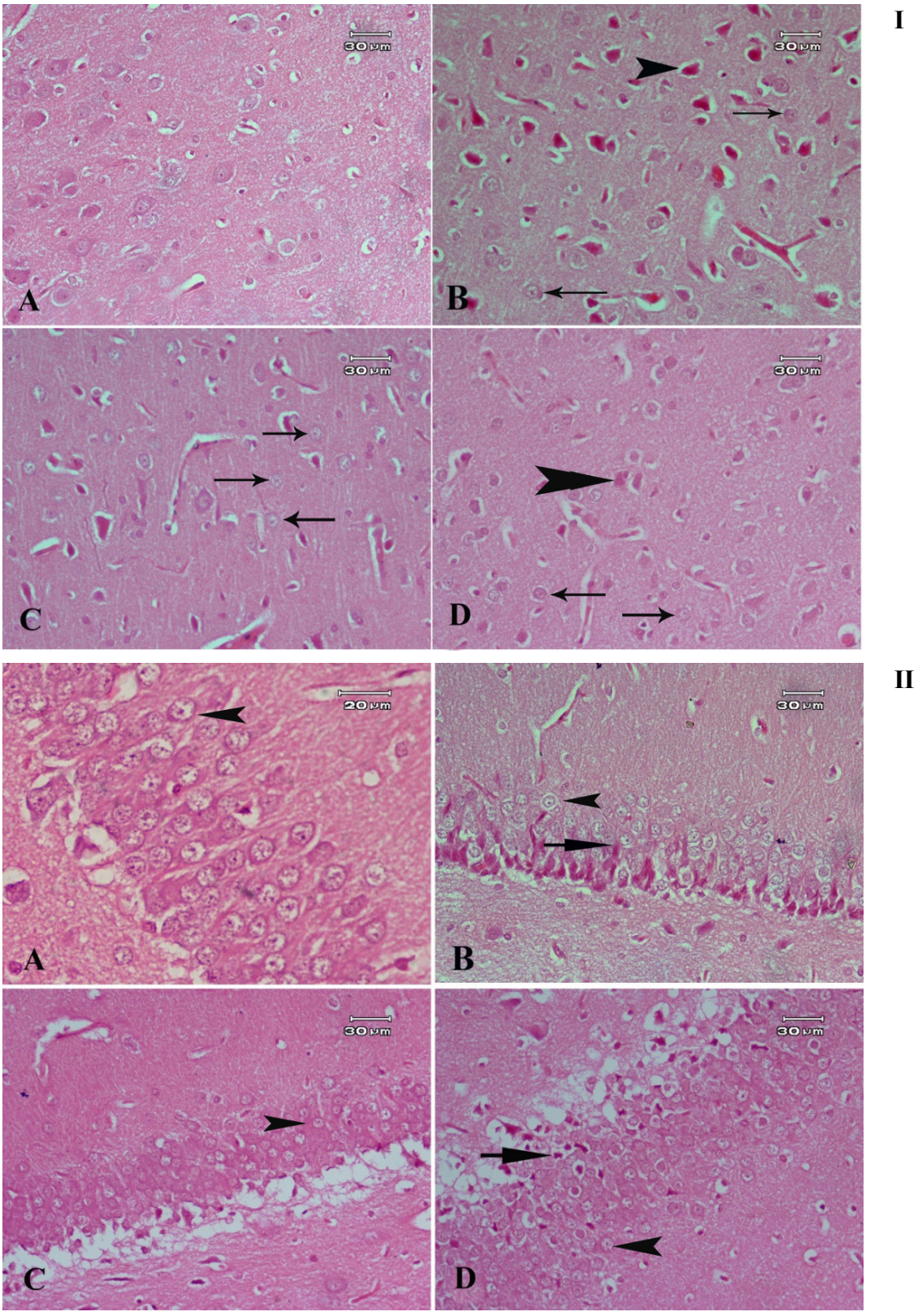

Fig. 5 (part I): A photomicrograph of cerebral cortex sections from the brain of: A) A normal control **rat. B)** A rat treated with STZ shows many small neurons with pyknotic nucleui and not well-defined nucleoli (arrowhead). **C)** A rat treated with Balanitis shows normally-shaped neurons (arrow). **D)** A rat treated with STZ and Balanitis shows only a few neurons with pyknotic nucleui (arrowhead). Most of the neurons appear normal in shape (arrow).

Fig. 5 (part II): A photomicrograph of sections of the hippocampal area from the brain of: A) A normal control rat shows normal neurons (arrow). **B)** A rat treated with STZ shows many small oval flattened neurons (arrow) among normal cells (arrowhead). **C)** A rat treated with Balanitis only shows a normal hippocampus area with normal neurons (arrowhead). **D)** A rat treated with STZ and Balanitis shows few neurons with pyknotic nuclei (arrow) with normal cells (arrowhead). The neurons are in a normally thick area.

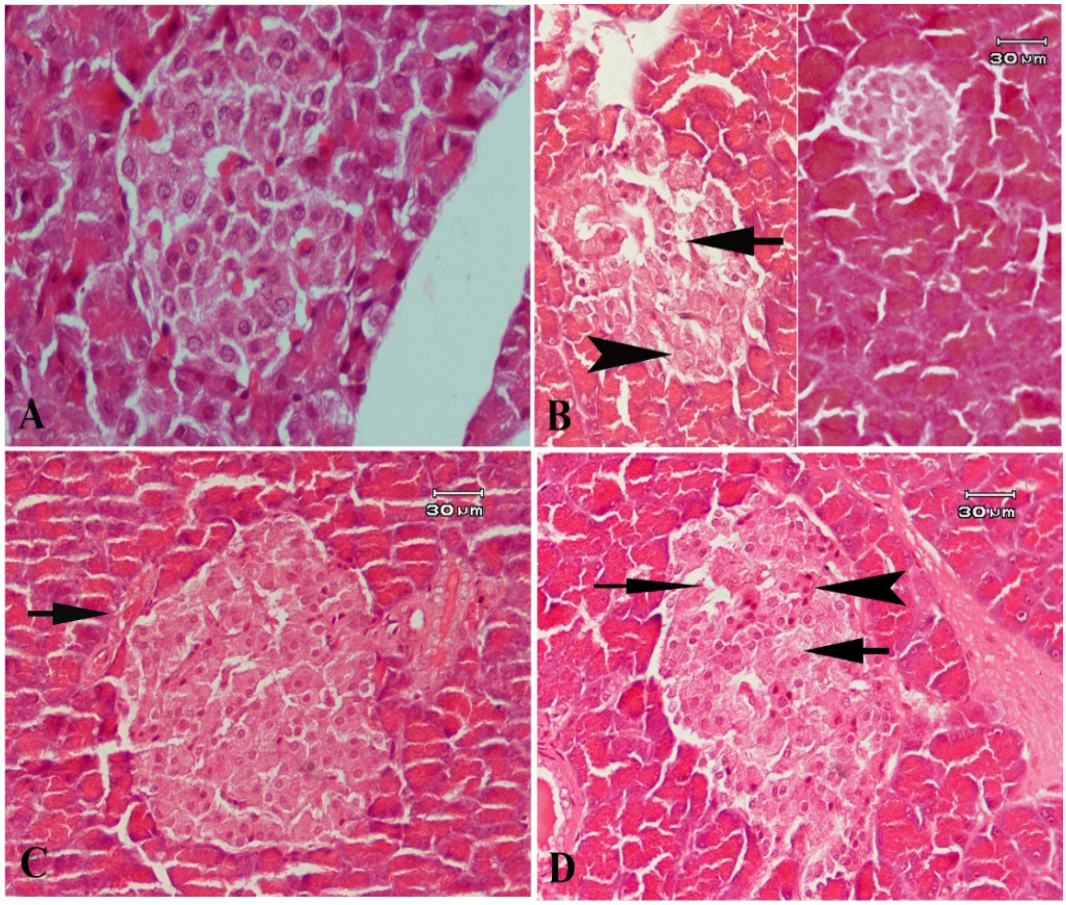

I

II

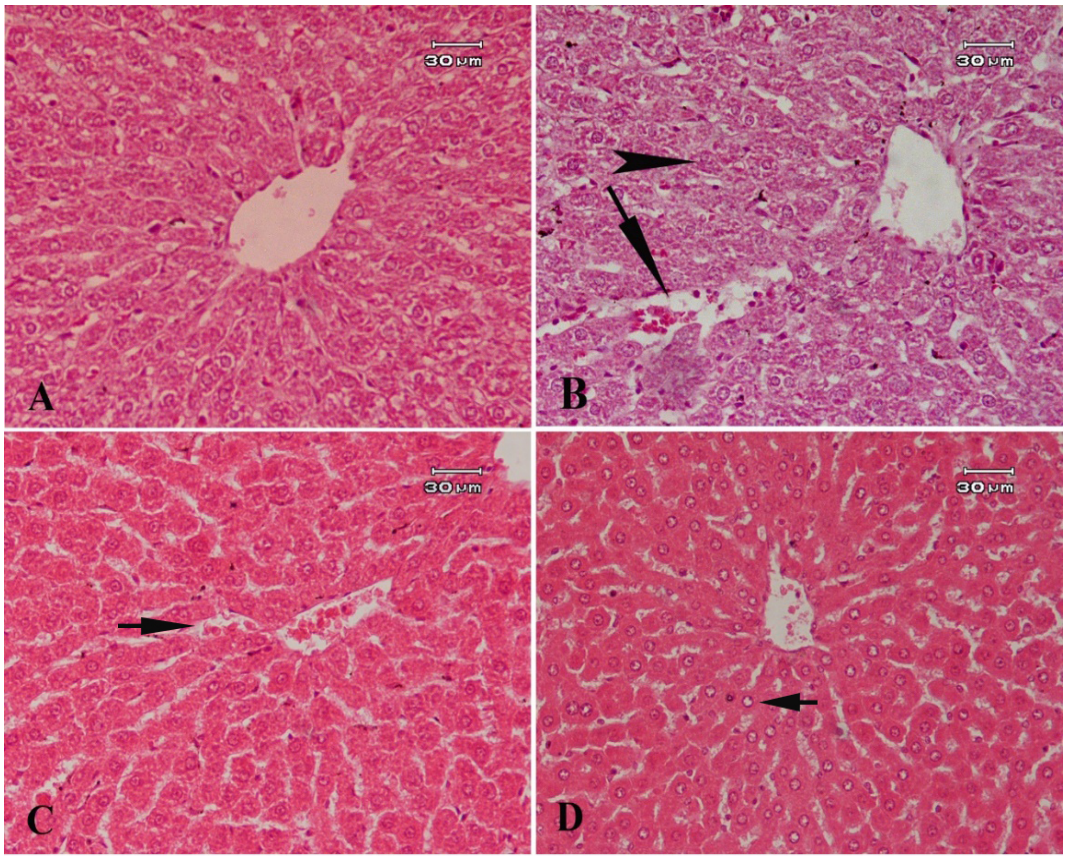

Fig. 6 (part I): A photomicrograph of sections of pancreatic tissue from:
A) A normal control rats. **B)** A STZ-treated rat shows apoptotic cells (arrow) and karyolysis (arrowhead). The other section shows a severe reduction of Langerhans islet's size. **C)** Normal rat treated with Balanitis shows slight congestion of blood vessels outside (arrow) normal size Langerhans islet. **D)** A rat treated with STZ & Balanitis shows very few apoptotic cells (arrowhead), increased fibrous component in between cells is also observed (arrow).

Fig. 6 (part II): A photomicrograph of sections of liver tissue from:
A) Normal control rat. **B)** A STZ-induced diabetic rat shows dilatation of blood sinusoids (arrow) and karyolysis of many cells (arrowhead). **C)** A normal rat treated with Balanitis shows slight congestion of blood vessels (arrow). **D)** STZ-induced diabetic rats treated with Balanitis show normal hepatic tissue appearance with healthy cells (arrow).

Immunohistochemical study

The examination of the brain sections of all groups stained immunohistochemically with anti-amyloid β antibody revealed that STZ had a damaging effect on brain tissue, which appeared as multiple positively stained areas in the cerebral cortex, denoting the presence of amyloid plaques **(Fig.7 [part I], B)**. The negative group **(Fig. 7 [part I], A)** and the extract group (**Fig. 7 [part I], C)** clarified the safety of the extract for brain tissue via the absence of positively stained areas. By examining the samples of the treated group, the extract has an ameliorating effect on the STZ-damaging effect as shown by the marked reduction of the positively stained areas in the cerebral cortex tissue **(Fig. 7 [part I], D).**

The examination of the hippocampal area of all groups obtained similar results, as negative staining results were observed in the negative group **(Fig. 7 [part II], A)** and the extract group **(Fig. 7 [part II], C),** denoting the safe use of *Balanitis* extract. Many positively stained areas were identified in animal sections of the
STZ group, indicating the damaging effect of this compound on the hippocampus **(Fig. 7 [part II], B).** Notable reduction in the positively stained areas was also observed in sections of the treated group, denoting the ameliorating effect of the extract **(Fig. 7 [part II], D).**

By examining pancreatic tissue stained immunohistochemically with anti-insulin antibody, sections from the negative group showed a strong positive reaction to the stain at the sites of insulin-secreting cells **(Fig. 7, A).** In addition, sections from the extract group showed a positive reaction to the

stain, which indicates the safe use of the extract for pancreatic tissue **(Fig. 7, C).** A negative reaction to the stain was observed in sections of the STZ group, denoting the destroying effect of this compound on insulin-secreting cells **(Fig. 7, B)**. Regaining positive reaction to stain was identified in sections of the treated group, denoting the return of insulin-secreting activity in this group of animals **(Fig. 7, D)**.

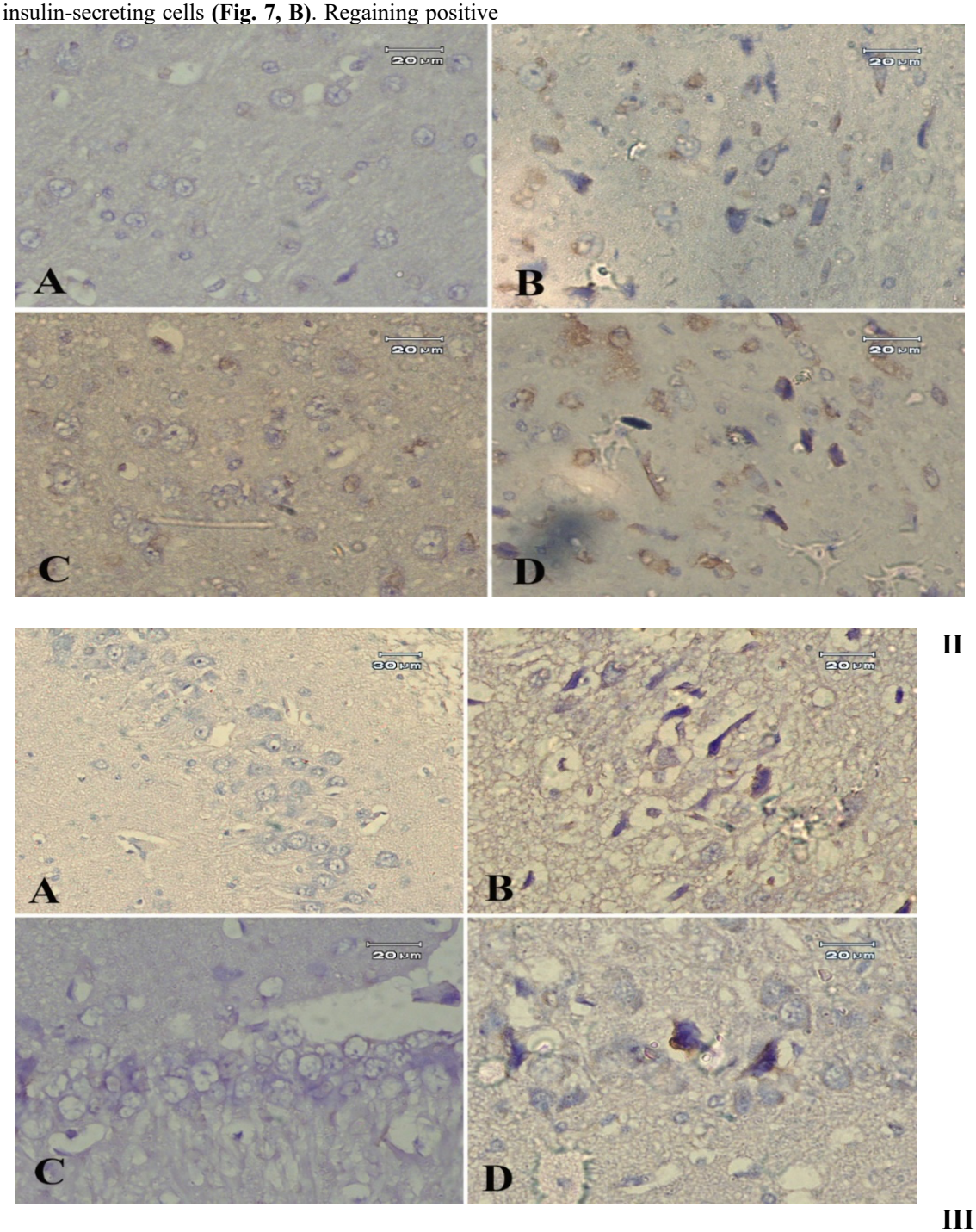

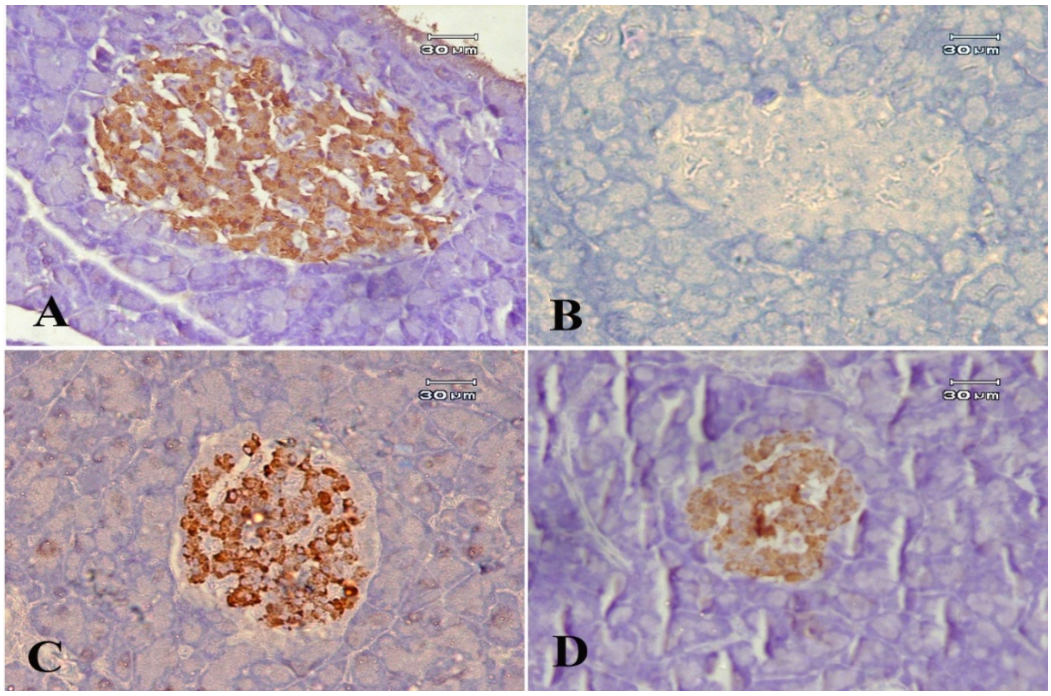

Fig. 7 (part I): A photomicrograph of cerebral cortex sections from the brain stained immunohistochemically by polyclonal Aβ antibody taken from:
A) A normal control rat shows a negative result. **B)** A rat treated with STZ shows multiple areas of positive reaction for the stain clarifying the presence of multiple amyloid plaques in the cerebral cortex of this group of animals. **C)** A normal rat treated with *Balanites* hydroethanolic extract shows a negative result for the stain. D) A rat treated with STZ and *Balanitis* extract shows a decrease of positively stained areas.
Fig. 7 (part II): A photomicrograph of sections of the hippocampal area stained immunohistochemically by polyclonal Aβ antibody from the brain of:
A) A normal control rat shows an adverse reaction to the stain. **B)** A rat treated with STZ shows many positively stained areas. **C)** A normal rat treated with *Balanites* dates hydroethanolic extract shows no positive reaction for the stain, which is close to normal. **D)** A rat treated with STZ and *Balanitis* shows a decrease of positively stained areas in the hippocampus.
Fig. 7 (part III): A photomicrograph of sections of pancreatic tissue stained immunohistochemically by anti-insulin antibody from:
A) A normal control rat shows a strong positive reaction to the stain all over the islet of Langerhan, which identify insulin-secreting cells. **B)** A rat treated with STZ shows negatively stained Islets of Langerhan with no noticeable reduction of Islets of Langerhan's size. **C)** A normal rat treated with *Balanites* dates hydroethanolic extract shows a reaction for the stain similar to a normal control rat. **D)** A rat treated with STZ and *Balanitis* shows a positive reaction of medium strength in many Langerhan's Islets. A reduction in the size of islets of Langerhan's is also observed.

Discussion

This study was conducted to discover the potential role of a natural anti-diabetic material in protecting the brain using a diabetes-induced neurodegenerative model. The current model was STZ-induced hyperglycemia in rats with diabetes neuro-complications. STZ injection produced remarkable hyperglycemia that illustrated a significant elevation in blood glucose and serum glucagon concentrations concurrent with a significant reduction in serum insulin and disruption in the serum lipid profile. In addition, STZ administration presented neurodegenerative disorders, where (i) AChE was activated, and ACh was decreased; (ii) Aβ and neurofibrillary tangles (NTF) occurrence; (iii) apoptosis was elevated with the decrease of Bcl-2, (iv) neuroinflammation occurred with the increase of IL-15, (v) BDNF was reduced, (vi) oxidative stress biomarkers (MDA, NO, and H_2O_2) were increased with a significant reduction in antioxidant biomarkers (GSH, GR, GST, GPx, SOD, and CAT).

Balanites, an anti-diabetic plant, showed anti-neurodegenerative properties, such as (i) significant inhibition in AChE, protecting ACh from hydrolysis; (ii) remarkable induction in BDNF; (iii) activation of anti-apoptotic factor (Bcl-2), (iv) significant decrease in neuroinflammatory marker (IL-15), (v) disappearance of Aβ and neurofibrillary tangles in the brain, and (vi) amelioration in oxidative stress compared with the STZ group. In addition, *Balanites* showed a significant reduction in blood glucose and serum glucagon concentrations, a

significant increase in serum insulin, and remarked amelioration in the serum lipid profile. These results were demonstrated by biochemical, histopathological, and immunohistochemical analyses.

Our obtained results on the anti-diabetic effect of *Balanites* fruits were agreed with **Kamel et al. [39], Gad et al. [40], Al-Malki et al. [41], and Hassanin et al. [42]. Kamel et al. [39]** confirmed the antidiabetic action of water extract of *Balanites* fruit in streptozotocin (STZ)-induced diabetic mice. They referred the antidiabetic activity of the extract to steroidal saponins, 26-O-ß-D-glucopyranosyl-(25R)-furost-5-ene-3ß,22,26-triol-3-O-[αL-rhamnophyranosyl-(1→1)]-[ß-D-xylopyranosyl-(1→3)]-[α-L-rhamnopyronosyl-(1→4)]- ß-D-glucopyranoside and its 22-methyl ether in the extract and recognized two additional saponins, 26-O-ß-D-glycopyranosyl-(25R)-furost-5-ene-3ß,22,26,-triol-3-O-[2,4-di-O-α-Lrhamnopyranosyl)-ß-D-glucopyranoside and its methyl ether. **Gad et al. [40]** reported that fruit hydroethanolic extracts caused a marked increment in the activity of glucose-6-phosphatase activity and decreased activity of glucose-6-phosphate dehydrogenase and phosphofructokinase in STZ-induced diabetic rats. Also, the extract recorded a reduction in blood glucose levels and significantly decreased liver glucose-6-phosphatase activity. The authors referred the activity to diosgenin, the major component in the extract. **Al-Malki et al. [41]** demonstrated the ability of ethyl acetate extract of *Balanites* fruit to modulate oxidative stress induced by streptozotocin due to the high content of β-sitosterol. Additionally, the recorded results on the antioxidant activities and anti-apoptotic effect of Balanites fruits were agreed with **Hassanin et al. [42].** They studied the effect of ethanolic extract of *Balanites* fruit and its butanolic and dichloromethane fractions on stress-activated protein kinase/c-Jun N-terminal kinase (SAPK-JNK) signaling in diabetic rats. *Balanites* materials caused a reduction in plasma glucose, hemoglobin A1c, lactic acid, lipid profile and MDA concentrations concurrent with significant increase in insulin and GSH concentrations and CAT and SOD activities. Also, apoptosis signal-regulating kinase 1, c-Jun N-terminal kinase 1 and protein 53 were down-regulated, meanwhile insulin receptor substrate 1 in rat pancreas and glucose transporter 4 were up-regulated in rat muscle. Fortunately, the anti-Alzheimer's effect of *Balanites* fruit in this study was agreed with our previous in-vitro study **Ibrahim er al. [8]**, where *Balanites* fruit hydroethanolic extract exhibited AChE and BuChE inhibitor action, as well as **El-Newary et al. [9]** where the same extract recorded Anti-Alzheimer's ability as we mentioned on the introduction section.

In the current study, *Balanites* prevented the progression of neurodegenerative disorders of diabetes that induce AD. The anti-neurodegenerative property of *Balanites* is shown on the basis of its potency to reduce (i) Aβ and NTF plaque, (ii) neuroinflammation, (iii) apoptosis, (iv) AChE activity, and (v) oxidative stress, which are all positively associated with hyperglycemia and insulin resistance. We discussed these phenomena based on the relationship between diabetes and neurodegenerative disorders, which have received significant attention. Several methods may cause diabetes-induced neurodegeneration, which will be discussed in the following sections.

High-glucose content in diabetes millets has significant toxicity on brain neurons. This toxicity occurred via osmatic insulin and oxidative stress. The preservation of chronically elevated glucose content also drives the induced formation of progressing glycation end products (AGEs), which have a potentially toxic effect on neurons. AGEs have been found in the central nervous system of individuals with diabetes. AGEs couple with free radicals and create oxidative damage, leading to neuronal injury. They also reactivate microglia in the CNS. Microglia, the resident innate immune cells in the brain, can be a deleterious and damaging factor. This process is considered as an underlying mechanism in diverse neurodegenerative diseases, including AD. Although microglia function is beneficial and mandatory for normal CNS functioning, they become toxic to neurons when over-activated and unregulated. In addition, AGEs induce amyloid oligomer deposition and participate in the formation of AD neurotoxicity. Concomitantly, tau glycation may promote the formation of double-helical filaments. The neurotoxicity of AGEs is illustrated by Sato et al. where AGEs reduce the cell viability of cortical neurons **[43-44]**. In the current study, *Balanites* administration significantly reduced the glucose level by about 51.83%, 58.75%, 67.23%, 66.33%, 67.57%, and 67.42% compared with the STZ group at 7, 14, 21, 30, 45, and 90 days, respectively, which could reduce or prevent the previously explained deleterious effect of glucose increment.

Insulin concentration*:* For a long time, it has been believed that the brain was an insulin-insensitive organ. The ability of insulin to cross the BBB lately came in the 1960s. The transport of insulin into BBB is reduced in insulin resistance–associated hyperinsulinemia, and insulin levels in the brain are subsequently lowered. Insulin and insulin receptors were found in the brain; the highest was in the olfactory bulb, cerebral cortex, hippocampus, cerebellum, and hypothalamus. However, a smaller proportion of insulin could be synthesized *de novo* in the brain **[45]**. Insulin exerts multidirectional activity in the brain, (i) providing nutrition, (ii) maintaining brain cell viability, (iii) improving synaptic functions,

(iv) blocking Aβ and neurofibrillary tangles, (v) improving learning and memory storage, (vi) and regulating brain's cerebral vasoreactivity **[46]**. Moreover, insulin involves learning and long-term memory storage by inducing the required MAPK signaling pathway. In addition, insulin induces NO production via inducing the endothelial nitric oxide synthase. NO is expressed in the hippocampus, and it participates in learning and synaptic plasticity **[45]**. Insulin signaling is also essential in synaptic plasticity by modulating glutamate and GABA receptors required for long-term memory consolidation **[47]**.

A recent study reported that insulin treatment reduces AChE activity in the hippocampal and frontal cortex regions of rats' brains. However, the same study demonstrated that acute hyperglycemia elevates AChE activity, but insulin administration reversed this effect **[48]**. Acetylcholine transferase (ChAT), an enzyme responsible for ACh synthesis, is expressed in insulin receptor-positive control neurons. Moreover, insulin regulates the ChAT expression **[49]**. In addition, activating PI3-K/Akt by insulin inhibits glycogen synthase kinase-3 (GSK-3). α form of GSK-3 regulates the formation of Aβ peptides. However, insulin regulates soluble AβPP release through the PI3-K-dependent pathway. Furthermore, insulin decreases intraneuronal Aβ deposition by accelerating AβPP/Aβ trafficking from the trans-Golgi network, a primary cellular site for Aβ generation, to the plasma membrane **[45]**. Under physiological conditions, a host of kinases and phosphatases regulate the intricate balance between tau phosphorylation and dephosphorylation to maintain neuronal homeostasis. However, under conditions of insulin resistance, GSK-3b hyperphosphorylates tau and decreases its affinity for microtubules which pretend the pre-tangles and NFTs in AD brains **[45-50]**. The relationship between ACh content and IGF was illustrated by **Rivera et al. [51]** who demonstrated the relationship between lower ChAT expression and IGF expression. In the clinical AD Braak stage, the mRNA associated with IGF-I, IGF-II, and their receptors and tau protein regulated by IGF-I and Hu D neuronal protein are decreased. Conversely, the increased Braak stage, gradually elevated Aβ concentrations, glial fibrillary acidic protein, and microglial transcripts were observed **[5]**.

Hyperinsulinemia also induces Aβ deposition. Insulin-degrading enzyme (IDE) is the enzyme that degrades insulin and Aβ protein. The two substrates compete on the enzyme. IDE is recognized as the Aβ regulator in neurons and glia. Hyperinsulinemia also elevates the insulin levels, which compete with Aβ for IDE, thereby suppressing the degradation of Aβ that progressively accumulates and forms insoluble plaques **[52]**. In general, insulin is vital for normal brain function. Therefore, disturbances in brain insulin function and insulin signal transduction have been associated with pathological conditions, including AD. *Balanites* administration for three months significantly increased insulin within normal ranges, indicating that neurodegenerative disorders were improved when insulin was elevated to acceptable ranges. Accordingly, (i) apoptosis was reduced with the significant increase in Bcl-2; (ii) Aβ and neurofibrillary tangle deposition were remarkably reduced based on histopathological studies; (iii) AChE was inhibited, and ACh content was significantly increased; (iv) cerebral circulation as sections of the brain was improved.

Dyslipidemia: Lipid metabolism is dependent on insulin. Therefore, any impairments in insulin signaling cause elevation in lipid deposition. About 30% of total body cholesterol is made in the human brain. Therefore, any changes in lipid metabolism could significantly affect cognitive function. In addition, Aβ synthesis and clearance must interact with cholesterol and Aβ precursor protein **[50]**. In the current study, STZ injection caused evident dyslipidemia, whereas *Balanites* administration showed significant improvement in this dyslipidemia. In particular, total cholesterol was significantly reduced. The current results indicated that the *Balanite*s hypocholesterolemic effect could prevent neurodegenerative induction or progression.

Oxidative stress: In mammalian cells, oxidation occurs typically in aerobic metabolism, but oxidation processes are considered "double-edged swords" that becomes harmful if not controlled. Type-2 diabetes and AD are oxidative stress–related diseases **[5]**. **De la Monte and Wands [5]** suggested that AD can be considered as type-3 diabetes. Oxidative stress activates enzymatic cascades at various cell compounds, including mitochondria, cytoplasm, and cell membranes, leading to cell damage and apoptosis. In preserving cell homeostasis, antioxidants, either enzymatic or non-enzymatic, are generated to maintain cell integrity and prevent injury and apoptosis. Although the powerhouses of cells are mitochondria, they are the critical organelle in producing ROS and RNS. Therefore, when mitochondria malfunction and produce a small amount of ATP, ROS and RNS production increases, as observed in AD and diabetes. Mitochondria reduce the production of free radicals through their uncoupling proteins in their inner membrane; this mechanism is inactive in brains with AD and diabetes. In addition, oxidative stress leads to neuronal injury through mitochondrial dysfunctions **[53]**. Diabetes represents alternations of the lipid profile, which lead cells to be more susceptible to lipid peroxidation. Moreover, the human brain is more susceptible to lipid peroxidation

because of its high content of polyunsaturated fatty acids **[44]**. Therefore, they are susceptible to oxidative stress. In this study, *Balanites* ameliorated the oxidative stress and depletion in antioxidant status associated with STZ injection. In addition*, Balanites* reduced lipid peroxidation (MDA) in the brain tissue, indicating its protective feature. Therefore, apoptosis and cell injury were decreased as shown in histopathological examination.

Inflammation: A mitochondrial malfunctioning is associated with insulin resistance in T2DM, exhibiting inflammation response. Inflammation induced augmentation in AGEs, tau, and Aβ deposition **[44]**. AGEs in T2DM are responsible for inducing Aβ deposition and cerebrovascular inflammation **[54]**. In addition, AGEs stimulate TNF-α, which accelerates β-secretase (BACE) expression, thereby inducing APP processing to form Aβ in astrocytes of diabetic models of AD **[55]**. In addition, inflammation represents Aβ-mediated activation of glial cells, which induces the formation of NFTs and apoptosis, leading to the progression of AD. Therefore, the incidence of AD is decreased in patients who consume non-steroidal anti-inflammatory drugs for pain or anti-diabetic drugs for peroxisome proliferator–activated receptor-G agonists **[44]**. Inflammation and cellular stress activate stress-sensitive kinases, some of which target eukaryotic initiation factor 2 alpha (eIF2a) and kinases involve in restoring homeostasis, namely, PKR, PERK, and GCN2. However, long-term brain metabolic stress and eIF2a kinase activity may lead to continually elevated eIF2a-P and accelerate neuronal injury similar to that observed in peripheral cells in diabetes. In addition, high eIF2a-P levels can upregulate activation transcription factor 4 expression, which is known as a propagator of neurotoxic signals in AD, Aβ production, and translational attenuation **[44]**. Notably, IL-15, as a pro-inflammatory cytokine, activates the glial cell. Microglial activation and microglia-derived oxidative stress have been described as critical processes in AD pathogenesis, which can lead to neurodegeneration **[56]**. Finally, diabetes-induced inflammation contributes to neurodegenerative disorders such as AD. In the current study, *Balanites* exhibited an anti-inflammatory effect, where IL-15 was significantly depleted, compared with STZ, which significantly increased this factor. In addition, our previous study **[9]** demonstrated the selective anti-inflammatory effect of *Balanites* against COX-2, not COX-1, required for cell maintenance. The obtained results indicate that *Balanites* administration for three months remarkably reduced diabetes-mediated inflammation in rats that could participates in the (i) reduction in Aβ and TNF deposition, (ii) inactivation in microglia, (iii) reduction in AGE production, (iv) recovery of mitochondrial function, and (v) decrease in apoptosis. These effects prevent memory impairment and behavioral outcomes of AD that collectively protect the brain from expected neurodegenerative diseases.

Finally, we could conclude that *Balanites* fruits hydroethanolic extract prevented the progression of neurodegenerative disorders of diabetes that induce AD. The anti-neurodegenerative property of *Balanites* is shown on the basis of its potency to reduce (i) Aβ and NTF plaque, (ii) neuroinflammation, (iii) apoptosis, (iv) AChE activity, and (v) oxidative stress, which are all positively associated with hyperglycemia and insulin resistance. These mentioned properties contributed to the chemical composition of the extract, which contains many active compounds that have been documented as anti-neurovegetative materials. These compounds are for example but not limited to kaempferol, myricetin, quercetin, gallic acid, and chlorogenic acid **[8-57]**.

Several studies have demonstrated the neuroprotective effect of **kaempferol**. Kaempferol can improve cognitive function through the inhibition of AChE activity in aluminum chloride-induced Alzheimer's Wistar rats models. In addition, kaempferol showed antioxidant action, which was responsible for reducing neurotoxic motor and cognitive injury in mice. In ovariectomized-streptozotocin- induced cognitive impairment, kaempferol significantly improved GSH and SOD, important against ROS-toxicity that is involved in the AD progression. Also, kaempferol reduced MDA, TNFα, and the cytochrome C apoptosis marker in the hippocampus of STZ- induced neurotoxicity in rats. 50 μM of kaempferol inhibited βA formation via blocking amyloid fibril elongation. kaempferol can suppress BV-2 microglia cells activation and its consequent neuroinflammatory toxicity via suppressing the activation of inflammatory pathways like toll-like receptor 4 (TLR4), factor nuclear kappa B (NF-κB), p38 mitogen-activated protein kinases (p38MAPK), and AKT **[58]**. **Myricetin** can prevent memory impairment in a rat model of AD induced by streptozotocin via reversing streptozotocin-induced reduction in neuronal numbers in the hippocampus. Myricetin can suppress memory disorders in D-galactose- induced AD in rat models by decrease in the phosphorylation levels of ERK1/2 and CREB, two molecules that have neuroprotective functions. *In-vitro*, myricetin promoted α-secretase expression and inhibited β-secretase activity, suggesting that promoting neuronal survival and inhibiting Aβ accumulation. Myricetin can reverse scopolamine-induced elevation in iron levels in the hippocampus in mice through direct chelating of intracellular Fe^{2+} or inhibition of transferrin receptor 1 (TrR1) expression, indicating that suppression of iron accumulation may contribute to the neuroprotective effects of myricetin in AD. Myricetin can avoid scopolamine-induced

increases in AChE activities, thereby inducing remarked raises in ACh contents in the hippocampus, suggesting that reversing cholinergic hypofunction may be a key mechanism for the anti-AD's effects of myricetin **[59]**. In transgenic AD mice model, **quercetin** considerably ameliorated neurodegeneration and cognitive and emotional deficits biomarkers. Quercetin regulated oxidative stress through reduction microglia aggregation around amyloid plaques in AD mice and inducing phosphoinositide 3-kinase (PI3K)/Akt that could down-regulate glycogen synthase kinase 3-beta (GSK-3b) activity, thereby reducing oxidative stress-mediated neuronal death. Quercetin modulated inflammatory response as suppression of LPS activated BV-2 microglial cells, by moderating the release of inflammatory mediators, as NO, TNF inducible NO synthase (iNOS). Quercetin regulated mitochondrial function by activating of AMP-activated protein kinase (AMPK), decreasing the phosphorylation of the eukaryotic initiation factor 2 alpha (eIF2a), activating the expression of transcription factor 4 (ATF4), resulting memory enhancement in aged mice and delayed memory deterioration at the early stage of APP23 AD model mice. Quercetin regulated autophagy function by maintaining the production of cell cycle protein as cell cycle proteins B. **[60]**. **Gallic acid** elevated the BDNF hippocampal level in AD patients. Gallic acid induced passive eschewal and memory function as well as promoted SOD, CAT, and GPx activities with reducing thiobarbituric acid (TBARS) concentrations substance in the hippocampus areas in intracerebroventricular- streptozotocin (STZ) induced AD rats **[61]**. **Xiong et al. [62]** reported that chlorogenic acid had an obvious ameliorating effect on neuroinflammation-induced cognitive dysfunction in in-vivo. **Chlorogenic acid** can inhibit microglial polarization toward the M1 phenotype and improve neuroinflammation-induced cognitive dysfunction in mice by modulating these key targets in the TNF signaling pathway.

Conclusions

This study demonstrated the relationship between anti-diabetic treatment and neurodegenerative disorder remediation. STZ injection induced neurodegeneration illustrated in a significant increase in AChE, Aβ, and neurofibrillary tangle deposition, which is related to AD. On the contrary, the administration of *Balanites* extracting diabetic animals for three months led to recovery from all these disorders. Finally, the potential anti-neurogenerative effect of *Balanites* extract is due to its anti-AchE, anti-apoptotic, antioxidant, and anti-neuroinflammation characteristics. Therefore, the current study can be generalized to a broader study population and clinical trials because *Balanitis* extract is entirely safe.

Author Contributions: Abeer Y. Ibrahim: Conceptualization, Supervision, Methodology, Investigation, Data curation, Formal analysis, Visualization, Validation, Software, Writing – original draft, and Writing – review & editing.
Nermeen M. Shaffie: Methodology, Investigation, Formal analysis, Visualization, Validation, Software, Writing – original draft, and Writing – review & editing. **Samah A. El-Newary:** Investigation, Methodology, Data curation, Formal analysis, Visualization, Validation, Software, Writing – original draft, and Writing – review & editing.
Funding: The National Research Centre funds this research work within the research budgets. No other funding was received from any other party that may affect the results directly or indirectly.
Informed Consent Statement: Not applicable.
Institutional Review Board Statement: The experiment was performed in Central Animal House of National Research Centre, Dokki, Egypt. The Medical Research Ethics Committee at National Research Centre, Egypt, approved this study under registration **No. 18/ 208**.
Availability of data and materials: All data generated or analyzed during this study are included in this published article.
Acknowledgments: The authors would like to sincerely thank National Research Centre, Egypt, for funding this research work within the research budgets. No other funding was received from any other party that may affect the results directly or indirectly.
Conflict of interest: The authors declare no conflict of interest.

References

[1] WHO, 2020. Egypt: Alzheimer's and dementia.
[2] Monteiro, F.; Sotiropoulos, I.; Carvalho, Ó.; Sousa, N.; Silva, F.S. Multi-mechanical waves against Alzheimer's disease pathology: a systematic review. *Transl. Neurodegener*. 2021, 10, 36 pages. https://doi.org/10.1186/s40035-021-00256-z.
[3] Gao, L.; Zhang, Y.; Sterling, K.; Song, W. Brain-derived neurotrophic factor in Alzheimer's disease and its pharmaceutical potential. *Transl. Neurodegener.* 2022, 11, 1–34. https://doi.org/org/10.1186/s40035-022-00279-0
[4] Confettura, A.D.; Cuboni, E.; Ammar, M.R.; Jia, S.; Gomes, G.M.; Yuanxiang, P.A.; et al. Neddylation-dependent protein degradation is a nexus between synaptic insulin resistance, neuroinflammation and Alzheimer's disease. *Transl. Neurodegener*. 2022, 11, 18 pages. https://doi.org/org/10.1186/s40035-021-0027.
[5] De la Monte, S.M.; Wands, J.R. Alzheimer's disease is Type 3 diabetes—evidence reviewed. *J. Diabetes Sci. Technol.* 2008, 2, 1101–1113. https://doi.org/10.1002/jcu.22334.
[6] Peng, X.; Fan, R.; Xie, L.; Shi, X.; Dong, K.; Zhang, S., et al. A growing link between circadian rhythms, Type 2 diabetes mellitus and Alzheimer's disease. *Int. J. Mol. Sci.* 2022, 23, 25 pages. https://doi.org/10.1161/CIRCULATIONAHA.115.016520
[7] De Sousa, R.A.L.; Harmer, A.R.; Freitas, D.A.; Mendonça, V.A.; Lacerda, A.C.R.; Leite, H.R. An update on potential links between type 2 diabetes mellitus and Alzheimer's disease. *Mo.l Biol. Rep.* 2020, 47, 6347-6356. doi: 10.1007/s11033-020-05693-z.
[8] Ibrahim, A.Y.; El-Newary, S.A.; Hendawy, S.F., Ibrahim, A.E. *Balanites aegyptiaca* extract to treat risk factors of Alzheimer's disease: An in vitro study. *Egypt J. Chem.* 2021, 64, 781–792.
[9] El-Newary, S.A., Youness, E.R., Shaffie, N.M., Ibrahim, A.Y. Anti-Alzheimer's potential role of *Balanites aegyptiaca* dates hydroethanolic extract in aluminum chloride model-induced neuronal toxicity in male albino rats. In press.
[10] OECD. OECD Guidelines for the testing of chemicals No. 423: acute oral toxicity-acute toxic class method; OECD: Paris, France, 1996.

[11] Abdel-Haleem, S.A., Ibrahim, A.Y., Ismail, R.F., Shaffie, N.M., Hendawy, S.F., Omer, E.A. *In-vivo* hypoglycemic and hypolipidemic properties of *Tagetes lucida* alcoholic extract in streptozotocin-induced hyperglycemic Wistar albino rats. *Ann. Agric. Sci.* 2017, 62, 169-181. https://doi.org/10.1016/j.aoas.2017.11.005.

[12] Van Pelt, L.F. Ketamine and xylazine for surgical anesthesia in rats. *J. Am. Vet. Med.* Assoc. 1977, 171, 842-844.

[13] Belfield, A.; Goldberg, D.M. Application of a continuous spectrophotometric assay for 5'nucleotidase activity in normal subjects and patients with liver and bone disease. *Clin. Chem*. 1969, 15, 931-939

[14] Rettman, S.; FrankelL, S. A colorimetric method for the determination of serum glutamic oxalacetic and glutamic pyruvic transaminases. *Am. J. Clin. Pathol.* 1957, 28, 56-63. https://doi.org/10.1093/ajcp/28.1.56

[15] Henry, R.J. Clinical chemistry, Principles and Techniques. Hoeber Medical, Harper-Row, 1964.

[16] Doumas, B.T.; Watson, W.A.; Biggs, H.G. Albumin standards and the measurement of serum albumin with bromcresol green. *Clin. Chim. Acta.* 1971, 258, 21-30. https://doi.org/10.1016/S0009-8981(96)06447-9.

[17] Reinhold, J.G. Standard methods in clinical chemistry. Academic Press, New York, 1953.

[18] Tabacco, A.; Meiattini, F.; Moda, E.; Tarli, P. Simplified enzymic/colorimetric serum urea nitrogen determination. *Clin. Chem.* 1979, 25, 336-337.

[19] Gochman, N.; Schmitz, J.M. Automated determination of uric acid. *Clin. Chem.* 1971, 17, 1154-1159.

[20] Faulkner, W.R.; King, J.W. Renal function. *Pol. Arch. Med. Wewn.* 1976, 975-1014.

[21] Allain, C.C.; Poon, L.S.; Chan, C.S.; Richand, W.; Paul, C.F. Enzymatic determination of total cholesterol. *Clin. Chem.* 1974, 20, 470-474.

[22] Naito, H.K.; Kaplan, A.Q. High-density lipoprotein (HDL) cholesterol. *Methods Clin. Chem.* 1984, 437, 1207-1213.

[23] Fossati, P.; Prencipe, L. Enzymatic determination of triglycerides. *Clin. Chem.* 1982, 28, 2077.

[24] Estadella, D.; Oyama, L.M.; Dâmaso, A.R.; Ribeiro, E.B.; Claudia, M.; Oller, D.N. Effect of palatable hyperlipidemic diet on lipid metabolism of sedentary and exercised rats. *Nutrition.* 2004, 20, 218-224.

[25] Friedewald, W.T.; Levy, R.I.; Fredrickson, D.S. Estimation of the concentration of Low-density lipoprotein cholesterol in plasma. *Clin. Chem*. 1972, 18, 499-502. https://doi.org/10.1177/107424840501000106.

[26] Montgomery, H.A.C.; Dymock, J. The determination of nitrite in water. *Analyst.* 1961, 86, 414-416.

[27] Chance, B.; Maehly, A.C. Assay of catalase and peroxidases. *Method Enzym*. 1955, 11, 764-775. https://doi.org/10.1002/9780470110171.ch14.

[28] Ohkawa, H.; Ohishi, N.; Yagi, K. Assay for lipid peroxides in animal tissues by thiobarbituric acid reaction. *Anal. Biochem*. 1979, 95, 351-358. https://doi.org/10.1016/0003-2697(79)90738-3.

[29] Griffith, O.W. Determination of glutathione and glutathione disulfide using glutathione reductase and 2-vinyl pyridine. *Anal. Biochem.* 1980, 106, 207-212. https://doi.org/10.1016/0003-2697(80)90139-6.

[30] Goldberg, D.M.; Spooner, R.J. Glutathione reductase. In: H. U. Bergmeyer, J. Bergmeyer and M. GraBI, Eds. In: Methods of Enzymatic Analysis, 3rd Editio. Verlag Chemie, Weinheim, 1983, pp; 258-265.

[31] Paglia, D.E.; Valentine, W.N. Studies on the quantitative and qualitative characterization of erythrocyte glutathione peroxidase. *J. Lab. Clin. Med.* 1967, 70, 158-169. https://doi.org/10.5555/uri:pii:0022214367900765.

[32] Habig, W.H.; Pabst, M.I.; Jacoby, W.B. Glutathione-S-transferase. *J. Biol. Chem.* 1974, 249, 7130-7139.

[33] Beers, R.F.; Sizer, I.W. A spectrophotometric method for measuring the breakdown of hydrogen peroxide by catalase. *J. Biol. Chem.* 1952, 195, 133-40. https://doi.org/10.1002/9780470110171.ch14.

[34] Fridovich, I. Superoxide dismutases. *Adv. Enzym. Relat. Areas. Mol. Biol.* 1974, 41, 35-97. https://doi.org/10.1002/9780470122860.ch2.

[35] Sedlak, J.; Lindsay, R.H. Estimation of total, protein-bound, and nonprotein sulfhydryl groups in tissue with Ellman's reagent. *Anal. Biochem.* 1968, 25, 192-205. https://doi.org/10.1016/0003-2697(68)90092-4.

[36] Drury, R.A.B.; Wallington, F.A. Corleton's histological technique. 4th Ed. Oxford, New York, Toronto, Oxford University Press, 1980.

[37] Murayama, H.; Shin, R.W.; Higuchi, J.; Shibuya, S.; Muramoto, T.; Kitamoto, T. Interaction of aluminum with PHFtau in Alzheimer's disease neurofibrillary degeneration evidenced by desferrioxamine-assisted chelating autoclave method. *Am. J. Pathol.* 1999, 155, 877- 885.

[38] Shin, R.W.; Ogino, K.; Shimabuku, A.; Taki, T.; Nakashima, H.; Ishihara, T.; Kitamoto, T. Amyloid precursor protein cytoplasmic domain with phospho-Thr668 accumulates in Alzheimer's disease and its transgenic models: a role to mediate interaction of A and tau. *Acta. Neuropathol.* 2007, 113, 627-636.

[39] Kamel, M.S.; Ohtani, K.; Kurokawa, T.; Assaf, M.H.; El-Shanawany, M.A.; Ali, A.A.; Kasai, R.; Ishibashi, S.; Tanaka, O. Studies on Balanites aegyptiaca fruits, an antidiabetic Egyptian folk medicine. Chem. Pharm. Bull. 1991, 39, 1229–1233.

[40] Gad, M.Z.; El-Sawalhi, M.M.; Ismail, M.F.; El-Tanbouly, N.D. Biochemical study of the antidiabetic action of the Egyptian plants Fenugreek and Balanites. Mol. Cell. Biochem. 2006, 281, 173–183.

[41] Al-Malki, A.L.; Barbour, E.K.; Abulnaja, K.O.; Moselhy, S.S. Management of hyperglycaemia by ethyl acetate extract of Balanites aegyptiaca (Desert date). Molecules 2015, 20, 14425–14434.

[42] Hassanin, K.M.A.; Mahmoud, M.A.; Hassan, H.M.; Abdel-Razik, A.H.; Aziz, L.N.; Rateb, M.E. Balanites aegyptiaca ameliorates insulin secretion and decreases pancreatic apoptosis in diabetic rats: Role of SAPK/JNK pathway. Biomed. Pharmacother. 2018, 102, 1084–1091.

[43] Sato, T.; Shimogaito, N.; Wu, X.; Kikuchi, S.; Yamagishi, S.; Takeuchi, M. Toxic advanced glycation end products (TAGE) theory in Alzheimer's disease. *Am. J. Alzheimer's Dis. Dementias.* 2006, 21, 197-208. https://doi.org/10.1177/1533317506289277

[44] Kandimalla, A.R.; Reddy, V.T.H. Is Alzheimer's disease a type 3 diabetes? a critical appraisal. *Biochim. Biophys. Acta. J.* 2017, 1863, 1078-1089. https://doi.org/.org/10.1016/j.bbadis.2016.08.018.

[45] Correia, S.C.; Santos, R.X.; Perry, G.; Zhu, X.; Moreiraa, P.I.; Smith, M.A. Insulin-resistant brain state: the culprit in sporadic Alzheimer's disease? *Ageing Res. Rev.* 2011, 10, 264-273. https://doi.org/10.1016/j.arr.2011.01.001.

[46] Cardoso, S.; Correi, S.; Santos, R.X.; Carvalho, C.; Santos, M.S.; Oliveira, C.R., et al. Insulin is a two-edged knife on the brain. *J. Alzheimer's Dis.* 2009, 18, 483-507. https://doi.org/10.3233/JAD-2009-1155 IOS.

[47] Van Der Heide, L.P.; Ramakers, G.M.J.; Smidt, M.P. Insulin signaling in the central nervous system: learning to survive. *Prog. Neurobio.* 2006, 79, 05-221. https://doi.org/10.1016/j.pneurobio.2006.06.003

[48] Jamshidnejad-Tosaramandani, T.; Kashanian, S.; Babaei, M.; Al-Sabri, M.H.; Schiöth, H.B. The potential effect of insulin on AChE and its interactions with rivastigmine *in vitro*. *Pharmaceuticals.* 2021, 14, 11 pages. https://doi.org/org/10.3390/ph14111136

[49] Umegaki, H. Neurodegeneration in diabetes mellitus. Chapter 19In: *Neurodegener. Dise.* 2012, 258-265.

[50] Chatterjee, S.; Mudher, A. Alzheimer's disease and type 2 diabetes: a critical assessment of the shared pathological traits. 2018, 12, 23 pages. https://doi.org/doi: 10.3389/fnins.2018.00383.

[51] Rivera, E.J.; Goldin, A.; Fulmer, N.; Travares, R.; Wands, J.R.; de La Monate, S.M. Insulin and insulin-like growth factor

expression and function deteriorate with progression of Alzheimer's disease: link to brain reductions in acetylcholine. *J. Alzheimers dis.* 2005, 8, 247-268. DOI: 10.3233/JAD-2005-8304

[52] Mullins, R.J.; Diehl, T.C.; Chia, C.W.; Kapogiannis, D. Insulin resistance as a link between amyloid-Beta and Tau pathologies in Alzheimer's disease. *Front. Aging Neurosci.* 2017, 9, 16 pages. https://doi.org/10.3389/fnagi.2017.00118

[53] Rousset, S.; Alves-Guerra, M.C.; Mozo, J.; Miroux, B.; Cassard-Doulcier, A.M.; Bouillaud, F.; Ricquier, D. The biology of mitochondrial uncoupling proteins. *Diabetes.* 2004, 53, 130-135

[54] Takeda, S.; Sato, N.; Uchio-Yamada, K.; Sawadac, K.; Kuniedac, T.; Takeuchia, D.; Kurinamia, H.; Shinoharaa, M.; Rakugib, H.; Morishita, R. Diabetes-accelerated memory dysfunction via cerebrovascular inflammation and Aβ deposition in an Alzheimer mouse model with diabetes. *Proc. Natl. Acad. Sci. USA.* 2010, 107, 7036-7041. https://doi.org/10.1073/pnas.1000645107.

[55] Ramasamy, R.; Yan, S.F.; Schmid,t A.M. Receptor for AGE (RAGE): Signaling mechanisms in the pathogenesis of diabetes and its complications. *Ann. N. Y. Acad. Sci.* 2011, 1243, 88-102. https://doi.org/10.1111/j.1749-6632.2011.06320.x.

[56] Gomez-Nicola, D.; Valle-Argos, B.; Pita-Thomas, D.W.; Nieto-Sampedro, M. Interleukin 15 expression in the CNS: blockade of its activity prevents glial activation after an inflammatory injury. *Glia*. 2008, 56, 494-505.

[57] Murthy, H.N.; Yadav, G.G.; Dewir, Y.H.; Ibrahim, A. Phytochemicals and Biological Activity of Desert Date (Balanites aegyptiaca (L.) Delile). Plants 2021, 10, 32. https://dx.doi.org/10.3390/plants10010032

[58] Silva dos Santos J, Gonçalves Cirino JP, de Oliveira Carvalho P and Ortega MM (2021) The Pharmacological Action of Kaempferol in Central Nervous System Diseases: A Review. Front. Pharmacol. 11:565700. doi: 10.3389/fphar.2020.565700.

[59] Li J, Xiang H, Huang C and Lu J (2021) Pharmacological Actions of Myricetin in the Nervous System: A Comprehensive Review of Preclinical Studies in Animals and Cell Models. Front. Pharmacol. 12:797298. doi: 10.3389/fphar.2021.797298.

[60] Cui Z, Zhao X, Amevor FK, Du X, Wang Y, Li D, Shu G, Tian Y and Zhao X (2022) Therapeutic application of quercetin in aging-related diseases: SIRT1 as a potential mechanism. Front. Immunol. 13:943321. doi: 10.3389/fimmu.2022.943321

[61] Shimul Bhuia, Mizanur Rahaman, Tawhida Islam, Mehedi Hasan Bappi , Iqbal Sikder, Kazi Nadim Hossain, Fatama Akter, Abdullah Al Shamsh Prottay, Rokonuzzman, Eda Sönmez Gürer, Daniela Calina, Muhammad Torequl Islam, Javad Sharif-Rad. Neurobiological effects of gallic acid: current perspectives. Chinese Medicine (2023) 18:27 https://doi.org/10.1186/s13020-023-00735-7

[62] Xiong S, Su X, Kang Y, Si J, Wang L, Li X and Ma K (2023) Effect and mechanism of chlorogenic acid on cognitive dysfunction in mice by lipopolysaccharide-induced neuroinflammation. Front. Immunol. 14:1178188. doi: 10.3389/fimmu.2023.1178188.